Doctoral Dissertation

Exploring partial restoration of chiral symmetry in nuclear matter by means of charmed mesons

チャームクォークを含む中間子を用いた核物質中でのカイラル対称性の部分的回復の探求

Daiki Suenaga

Department of Physics,
Nagoya University

Supervisor: Professor Masayasu Harada

January 2018

Abstract

Chiral symmetry is spontaneously broken in the vacuum and hadron masses and pion dynamics are understood in a unified way. This symmetry is, however, expected to be restored at high density. In this dissertation, I focus on charmed mesons such as $\bar{D}$ mesons as probes for exploring the change of chiral symmetry in nuclear matter. Nuclear matter is described by a chiral model such as a linear sigma model or a parity doublet model, and $\bar{D}$ mesons are introduced by a chiral partner structure. In the context of the chiral partner, a mass difference between positive-parity meson and negative-parity meson is generated by the spontaneous breakdown of chiral symmetry so that I especially investigate masses and spectral functions for $\bar{D}_0^*$ (0^+) and $\bar{D}$ (0^-) mesons in nuclear matter respecting chiral symmetry.

First, I study density dependences of the masses and spectral functions for $\bar{D}_0^*$ and $\bar{D}$ meson in the low density region within the linear sigma model. The results show that the mass of $\bar{D}$ meson increases while that of $\bar{D}_0^*$ meson decreases with increasing density which essentially reflects a partial restoration of chiral symmetry. In the spectral function for $\bar{D}_0^*$ meson, I find three peaks. The first peak is corresponding to a $\bar{D}_0^*$ resonance. This peak shifts to the lower energy regime as we increase the density which shows the reduction of its mass, and gets broadened by a collisional broadening. The second peak is regarded as a threshold enhancement. This peak shifts to the higher energy regime as the density increases and gets remarkably enhanced so that this peak is a proper probe for observing the partial restoration of chiral symmetry in nuclear matter. The third peak is a Landau damping and this peak gradually grows as we increase the density.

Next, I study the chiral invariant mass dependence of spectral function for $\bar{D}_0^*$ meson at the normal nuclear matter density within the parity doublet model. I find two clear peaks regarded as a resonance of $\bar{D}_0^*$ meson and a threshold enhancement. As we increase the value of chiral invariant mass, the peak position of $\bar{D}_0^*$ meson resonance shifts to the lower energy regime while that of the threshold enhancement shifts to the higher energy regime. These changes, especially the threshold enhancement, provide us with fruitful information on the value of the chiral invariant mass as well as the magnitude of partial restoration of chiral symmetry in nuclear matter.

Contents

Chapter 1

Introduction

Hadrons such as nucleon and pion are understood as composite particles made by plural quarks, and their binding mechanism is dominated by Quantum Chromodynamics (QCD). However, QCD dynamics is non-perturbative at low energy regime with its complicated non-abelian interactions. As a result, comprehensive understanding of hadron properties and interactions by an *ab-initio* calculation is extremely difficult. Because of this difficulty, it is appropriate to understand hadron interactions at hadronic level. An effective field theory (or an effective model) is enumerated as one of such methods. In this procedure, an effective Lagrangian for hadrons is constructed by respecting symmetries of QCD to fully respect the original theory. Therefore, "symmetry" is a keyword in this dissertation.

QCD possesses approximate chiral symmetry since quark masses are greatly suppressed in comparison with $\Lambda_{\rm QCD}$ [1]. This suggests that the spontaneous breakdown of chiral symmetry is one of the most powerful scenarios to give clues to answer the question of mass generation of a nucleon as with Higgs mechanism in Glashow-Weinberg-Salam theory [1, 2, 3, 4]. In this context, pions are regarded as Nambu-Goldstone bosons (NG bosons) [5, 6]. Pion dynamics and interaction manners with the nucleon are actually well described by low energy theorems in association with the spontaneous breakdown of chiral symmetry [8, 7].

Chiral symmetry is undoubtedly spontaneously broken in QCD as stated above. It is discussed, however, that various changes of its phase are expected at temperature and/or density, e.g., partial restoration of chiral symmetry, emergence of inhomogeneous chiral broken phases, complete restoration of chiral symmetry, and so on [9]. These variations are so influential in hadron properties at such extreme

[1] Here I restrict our discussion in two flavor case so that $m_q \sim O(1)$ MeV while $\Lambda_{\rm QCD} \sim O(10^2)$ MeV.

environments that understanding of QCD phase diagram in terms of chiral symmetry is indispensable, e.g., in studying Heavy Ion Collision experiments and Neutron Star observations.

At temperature, a numerical *ab-initio* calculation called lattice QCD simulation is successfully applied, and chiral symmetry at temperature is now under the investigation [12]. In contrast, the lattice QCD simulation fails to run at density because of a disastrous problem so-called sign problem. Therefore, information on chiral symmetry at density is poor and an observation of partial restoration of chiral symmetry at density is still controversial (see Ref. [13] as a review and references therein).

In order to explore the chiral symmetry at density, I propose $\bar{D}\,(\sim \bar{c}q)$ meson can be an appropriate probe [14, 15, 16, 17, 18]. $\bar{D}$ meson is composed of one light quark and one anti-charm quark, then these mesons have two advantages:

(I) Thanks to the large mass of charm quark, $1/\Lambda_{\rm QCD}$ expansion is applicable.

(II) $\bar{D}$ meson belongs to the fundamental representation of chiral group.

From (I), a symmetry called " Heavy Quark Spin Symmetry (HQSS) " emerges, and a concise effective Lagrangian is constructible [19, 20]. The advantage (II) allows $\bar{D}$ mesons to interact with pions and other light mesons in an unsophisticated manner [21]. Note that I especially adopt $\bar{D}$ mesons but not D mesons to avoid complicated pair annihilation processes. $\bar{D}$ mesons in nuclear matter are expected to be realized at FAIR (Facility for Antiproton and Ion Research) and J-PARC (Japan Proton Accelerator Research Complex) in the future.

Previous studies on charmed mesons in nuclear matter by means of quark meson coupling model [22], QCD sum rule [23, 24, 25, 26, 27], coupled channel analysis [28, 29, 30, 31] and chiral effective model [17, 32, 33, 34] exist. Although some works on charmed mesons in nuclear matter based on the chiral effective model are published, it is not easy to include the tendency of the restoration of chiral symmetry explicitly since a self-consistent calculation in medium requires a terrible numerical computation. Therefore, I investigate $\bar{D}$ mesons in nuclear matter with the partial restoration of chiral symmetry fully respecting chiral symmetry by a chiral effective model in this dissertation. First, I employ the linear sigma model to describe nuclear matter since this model is one of the most concise effective models to represent the spontaneous breakdown of chiral symmetry and the mass generation of the nucleon [35, 36]. Next, the parity doublet model [37, 38] is applied to study $\bar{D}$ meson at the normal nuclear matter density quantitatively.

I utilize the chiral partner structure for constructing a Lagrangian for $\bar{D}$ mesons together with the HQSS [39, 40]. In this structure, a mass difference between positive-

parity $\bar{D}$ meson and negative-parity $\bar{D}$ meson is generated by the breakdown of chiral symmetry, which is a clear manifestation of advantage (II). In the real world, $\bar{D}$ (1869) (0^-) and $\bar{D}_0^*$ (2318) (0^+) meson are regarded as the partner while $\bar{D}^*$ (2010) (1^-) and $\bar{D}_1$ (2427) (1^+) meson are regarded as the partner. Furthermore, we can find a characteristic relation called the extended Goldberger-Treiman relation among them. For instance, the mass difference between $\bar{D}_0^*$ meson and $\bar{D}$ meson (Δ_m) is related to the $\bar{D}_0^*\bar{D}\pi$ coupling constant ($g_{\bar{D}_0^*\bar{D}\pi}$) by $\Delta_m = g_{\bar{D}_0^*\bar{D}\pi}\sigma_0$, with σ_0 being a mean field of σ meson. This relation claims that mass difference between the chiral partner gets small when we access to nuclear matter at which the chiral symmetry is expected to be partially restored. Accordingly, a visible mass shift of $\bar{D}_0^*$ meson and a change of width of $\bar{D}_0^*$ meson are expected in nuclear matter. Motivated by this prospect, I investigate the mass and spectral function for $\bar{D}_0^*$ meson as well as $\bar{D}$ meson in nuclear matter.

This dissertation is organized as follows: In Chap. 2, I construct an effective Lagrangian of $\bar{D}$ meson based on the HQSS and the chiral partner structure. In Sec. 3, I describe nuclear matter by the linear sigma model and study the partial restoration of chiral symmetry. In Chap. 4, I investigate masses and spectral functions for $\bar{D}$ and $\bar{D}_0^*$ mesons. In Chap. 5, I further construct nuclear matter by the parity doublet model and study a spectral function for $\bar{D}_0^*$ meson at normal nuclear matter density. Finally, in Chap. 6, I give conclusions.

Chapter 2

Heavy Meson Effective Theory

In this chapter, I construct an effective Lagrangian for $\bar{D}$ mesons. $\bar{D}$ meson contains an anti-charm quark whose mass is larger in comparison with the typical energy scale of QCD ($\Lambda_{\rm QCD}$), and this hierarchy allows us to construct an effective theory which is called "Heavy Quark Effective Theory (HQET)". In Sec. 2.1, I briefly show a derivation of HQET and appearance of the "Heavy Quark Spin Symmetry (HQSS)". In Sec. 2.2, I introduce heavy-light meson fields consistently with HQET. In Sec. 2.3, I give an explanation of an idea of chiral partner structure and construct an effective Lagrangian for $\bar{D}$ mesons which is based on the HQET and the chiral partner structure. This Lagrangian plays a central role in the later analysis.

2.1 Heavy Quark Effective Theory

Here I give a brief derivation of the Heavy Quark Effective Theory (HQET) [19, 20]. The propagator of a quark with momentum Q and mass m_Q is given by

$$\frac{i}{\not{Q} - m_Q + i\epsilon} \ . \tag{2.1}$$

By separating the momentum of quark Q as $Q^\mu = m_Q v^\mu + k^\mu$ with v being the "velocity" of the quark ($v^2 = 1$) and k being the residual momentum, and taking the quark mass to be infinity: $m_Q \to \infty$, the propagator of a quark (2.1) is reduced as

$$\begin{aligned} \frac{i}{\not{Q} - m_Q} &= \frac{i(m_Q \not{v} + \not{k} + m_Q + i\epsilon)}{(m_Q v + k)^2 - m_Q^2} \\ &\to \frac{1 + \not{v}}{2} \frac{i}{v \cdot k + i\epsilon} \ . \end{aligned} \tag{2.2}$$

Namely, the leading order of the HQET is defined by an effective Lagrangian which reproduces the propagator in Eq. (2.2).

The quark field ψ is decomposed into two ingredients as

$$\begin{aligned}\psi &= \mathrm{e}^{-im_Q v\cdot x}\left[\mathrm{e}^{im_Q v\cdot x}\frac{1+\not{v}}{2}\psi + \mathrm{e}^{im_Q v\cdot x}\frac{1-\not{v}}{2}\psi\right] \\ &\equiv \mathrm{e}^{-im_Q v\cdot x}\left[\psi_v + \Psi_v\right] \end{aligned} \tag{2.3}$$

where I have defined a large component ψ_v and a small component Ψ_v of the quark by

$$\psi_v = \mathrm{e}^{im_Q v\cdot x}\frac{1+\not{v}}{2}\psi \tag{2.4}$$

$$\Psi_v = \mathrm{e}^{im_Q v\cdot x}\frac{1-\not{v}}{2}\psi\ . \tag{2.5}$$

In these expressions, $\frac{1+\not{v}}{2}$ turns into $\frac{1+\gamma^0}{2}$ at the rest frame $v^\mu = (1,\vec{0})$ which is regarded as the projection operator picking up only the positive-energy part of the quark. In a similar manner, $\frac{1-\not{v}}{2}$ is regarded as the projection operator picking up only the negative-energy part of the quark.

By substituting the decomposition (2.3) into the original QCD Lagrangian, we find

$$\begin{aligned}\mathcal{L} &= \bar{\psi}(i\not{D} - m)\psi \\ &= \left(\bar{\psi}_v + \bar{\Psi}_v\right)\mathrm{e}^{imv\cdot x}(i\not{D} - m)\mathrm{e}^{-imv\cdot x}\left(\psi_v + \Psi_v\right) \\ &= (\bar{\psi}_v + \bar{\Psi}_v)i\not{D}(\psi_v + \Psi_v) - m(\bar{\psi}_v + \bar{\Psi}_v)(1-\not{v})(\psi_v + \Psi_v)\ . \end{aligned} \tag{2.6}$$

As we have seen in Eq. (2.2), the quark propagator contains only positive-energy part in the heavy quark limit $m_Q \to \infty$. Then we can simply drop the small component Ψ_v in Eq. (2.6) at the leading order, which reads

$$\begin{aligned}\mathcal{L} &= \bar{\psi}_v i\not{D}\psi_v - m\bar{\psi}_v(1-\not{v})\psi_v \\ &= \bar{\psi}_v\frac{1+\not{v}}{2}i\not{D}\frac{1+\not{v}}{2}\psi_v - m\bar{\psi}_v\frac{1+\not{v}}{2}(1-\not{v})\frac{1+\not{v}}{2}\psi_v \\ &= \bar{\psi}_v iv\cdot D\psi_v\ , \end{aligned} \tag{2.7}$$

where I have used a relation

$$\psi_v = \frac{1+\not{v}}{2}\psi_v\ . \tag{2.8}$$

From the reduced Lagrangian (2.7), the propagator is obtained as

$$\frac{i}{v \cdot k + i\epsilon} \ , \tag{2.9}$$

and using the relation in Eq. (2.8), this is completely identical to the heavy quark propagator (2.2). Therefore, the Lagrangian in Eq. (2.7) defines the HQET at the leading order.

The Lagrangian (2.7) shows that the interaction term between a heavy quark and a gluon does not include γ matrices so that heavy quark does not change its spin in the gluon emission process. Thanks to this magnificent feature, we find a global $SU(2)_S$ spin symmetry which is called the Heavy Quark Spin Symmetry (HQSS). This symmetry plays an important role in constructing a Heavy Meson Effective Theory as will be seen in Sec. 2.2. Note that the heavy quark has only its positive-energy component and the spin polarization is fixed, which manifestly shows that HQET is completely equivalent to a non-relativistic theory of QCD.

2.2 Heavy-light meson fields

In this section, I show how a heavy-light meson field can be introduced incorporating the HQET. When we consider a heavy-light meson which is composed of a heavy quark Q and an anti-light quark $\bar{q}$, we can regard it as if a cloud of the light degrees of freedom is surrounding the heavy quark (Brown Muck picture). From the standpoint of this picture, the heavy quark dominates the motion of the heavy-light meson, and the light anti-quark simply follows it.

The heavy-light meson should have a global $SU(2)_S$ spin symmetry referred to as the HQSS which showed up in Sec. 2.1. From the point of view of addition of spin, the spin representation of the heavy-light meson is

$$\mathbf{2}_h \otimes \mathbf{2}_l = \mathbf{3} \oplus \mathbf{1} \ , \tag{2.10}$$

where $\mathbf{2}_h$ and $\mathbf{2}_l$ correspond to the spin of heavy quark and anti-light quark, respectively. In Eq. (2.10), $\mathbf{3}$ obviously denotes the vector meson (1^-) while $\mathbf{1}$ denotes the pseudo-scalar meson (0^-). Thanks to the HQSS, masses of these two mesons degenerate. This feature is, however, realized in the heavy quark limit while masses of observed heavy-light mesons such as D mesons ($\bar{D} \sim c\bar{q}$) in the real world are not infinite. In fact, the HQSS is slightly violated due to the small mass difference between D (1870) (0^-) and D^* (2010) (1^-), however the mass splitting is suppressed by $O(\Lambda_{\rm QCD}/m_c)$ with m_c being the mass of a charm quark. Therefore, we can respect

the HQSS for D mesons as a first approximation. In the main analysis in Chap. 4 and Chap. 5, I will include the violation of HQSS. Note that the HQSS works better for bottom quark sector since its mass is heavier than that of charm quark, so that the mass degeneracy between $\bar{B}$ (5279) (0^-) and $\bar{B}^*$ (5325) (1^-) is well realized ($\bar{B} \sim b\bar{q}$).

The degeneracy of vector and pseudo-scalar meson suggests that it is more convenient to treat these mesons in a unified way. Keeping in mind this peculiarity, let us introduce a heavy-light meson field H_v parametrized as

$$H_v = \frac{1+\not{v}}{2}\left[\not{D}_v^* + i\gamma_5 D_v\right] \ . \tag{2.11}$$

$D_v^{*\mu}$ is a vector field and D_v is a pseudo-scalar field which are regarded as the observed D mesons. The subscript v represents that these fields are defined within the effective theory of heavy degrees of freedom. This H_v field is schematically indicated as

$$H^a_{v,hl} \sim c_h \bar{q}^a_l \ , \tag{2.12}$$

where h and l are the spin index of the charm quark and the light anti-quark, respectively, and a denotes the isospin degrees of freedom. The projection operator $\frac{1+\not{v}}{2}$ in Eq. (2.11) is needed so as to reproduce the reduction obtained in the HQET for the charm quark in (2.12). Under the parity transformation, D and D^* mesons transform as

$$\begin{aligned} D_v(x) &\xrightarrow{P} -D_v(x_p) \\ D^*_{v,\mu}(x) &\xrightarrow{P} D_v^{*\mu}(x_p) \ , \end{aligned} \tag{2.13}$$

where x_p refers to $x_p = (x^0, -\vec{x})$. Accordingly, heavy-light meson field H_v transforms in a simple manner as

$$\begin{aligned} H_v(x) &= \frac{1+\not{v}}{2}\left[\not{D}_v^*(x) + i\gamma_5 D_v(x)\right] \\ &\xrightarrow{P} \frac{1+\not{v}}{2}\left[D_v^{*\nu}(x_p)\gamma^\nu - i\gamma_5 D_v(x_p)\right] \\ &= \gamma^0 \frac{1+v^\mu\gamma^\mu}{2}\left[\not{D}_v^*(x_p) + i\gamma_5 D_v(x_p)\right]\gamma^0 \\ &= \gamma^0 H_{v_p}(x_p)\gamma^0 \ , \end{aligned} \tag{2.14}$$

which is consistent with the schematic picture in Eq. (2.12). Under the $SU(2)_S$ heavy quark spin transformation, H_v transforms as

$$H_v \ \to \ S_Q H_v \ , \tag{2.15}$$

where S_Q is an element of the $SU(2)_S$ HQSS. These transformation laws are necessary to construct an effective Lagrangian of heavy-light mesons as will be seen in Sec. 2.3.

2.3 Chiral partner structure for D mesons

In this section, I introduce a characteristic feature of D mesons ($\bar{D}$ mesons) related to chiral symmetry called the "chiral partner structure", and complete our construction of an effective Lagrangian for $\bar{D}$ mesons [39, 40]. The chiral partner structure claims that a mass difference between positive-parity state and negative-parity state is generated by the spontaneous breakdown of chiral symmetry.

Within the linear representation of light flavors, the schematic picture of heavy-light meson field (2.12) is described as

$$H_{v,L} \sim c\bar{q}_L \ , \quad H_{v,R} \sim c\bar{q}_R \ . \tag{2.16}$$

Then these fields transform under the $SU(2)_L \times SU(2)_R$ chiral transformation as

$$H_{v,L} \to H_{v,L} g_L^\dagger \ , \quad H_{v,R} \to H_{v,R} g_R^\dagger \ , \tag{2.17}$$

where g_L and g_R are elements of $SU(2)_L$ and $SU(2)_R$ chiral group, respectively. The transformation laws under the $SU(2)_S$ heavy quark spin transformation and parity transformation are identical to (2.15) and (2.14), respectively. By employing these transformation laws, we can easily construct an effective Lagrangian for D mesons which holds the $SU(2)_L \times SU(2)_R$ chiral symmetry, $SU(2)_S$ HQSS and parity as

$$\begin{aligned}
\mathcal{L}_{\rm HMET} \ = \ & {\rm tr}[H_{v,L}(iv\cdot\partial)\bar{H}_{v,L}] + {\rm tr}[H_{v,R}(iv\cdot\partial)\bar{H}_{v,R}] \\
& + \frac{\Delta_m}{2f_\pi}{\rm tr}[H_{v,L}M\bar{H}_{v,R} + H_{v,R}M^\dagger\bar{H}_{v,L}] \\
& + i\frac{g}{2f_\pi}{\rm tr}[H_{v,R}\gamma_5\gamma^\mu\partial_\mu M^\dagger\bar{H}_{v,L} - H_{v,L}\gamma_5\gamma^\mu\partial_\mu M\bar{H}_{v,R}] \\
& + \cdots \ .
\end{aligned} \tag{2.18}$$

$\bar{H}_{v,L(R)}$ is defined by $\bar{H}_{v,L(R)} = \gamma_0 H_{v,L(R)}^\dagger \gamma_0$. The chiral field M contains σ meson and pions parametrized as

$$M = \sigma + i\pi^a\tau^a \ , \tag{2.19}$$

where τ^a ($a = 1, 2, 3$) is the Pauli matrix. The quark contents of this field is indicated by

$$M^{ij} \sim \bar{q}_R^j q_L^i \ , \tag{2.20}$$

which leads to a transformation law under the $SU(2)_L \times SU(2)_R$ chiral transformation as [1]

$$M \to g_L M g_R^\dagger \ . \tag{2.21}$$

Δ_m and g are free parameters which will be determined soon, and f_π is the pion decay constant. The kinetic terms of heavy-light mesons in (2.18) are of the same form as that of a heavy quark in (2.7) motivated by the sense of Brown Muck picture described in Sec. 2.2. Note that in constructing the Lagrangian (2.18), We have remained up to first derivative terms and one chiral field M with an assumption that higher derivatives and multiple light meson couplings are suppressed.

$H_{v,L}$ and $H_{v,R}$ are so useful to construct the Lagrangian since the chiral representation is transparent. These fields, however, are not eigenstates of parity and are not corresponding to the observed heavy-light mesons. The interpolating fields in (2.16) are rewritten as

$$H_{v,L} \sim \frac{1}{2} c\bar{q} + \frac{1}{2} c\bar{q}\gamma_5 \tag{2.22}$$

$$H_{v,R} \sim \frac{1}{2} c\bar{q} - \frac{1}{2} c\bar{q}\gamma_5 \ , \tag{2.23}$$

which suggests that the parity eigenstates H_v and G_v which contain $(0^-, 1^-)$ and $(0^+, 1^+)$, respectively, can be related as

$$\begin{aligned} H_{v,L} &= \frac{1}{\sqrt{2}}(G_v + iH_v\gamma_5) \\ H_{v,R} &= \frac{1}{\sqrt{2}}(G_v - iH_v\gamma_5) \ , \end{aligned} \tag{2.24}$$

for example. D (0^-) and D^* (1^-) mesons belong to H_v while D_0^* (0^+) and D_1 (1^+) mesons belong to G_v, so that H_v and G_v are parametrized with an analogy in Eq. (2.11) as

$$\begin{aligned} H_v &= \frac{1+\not{v}}{2}[i\gamma_5 D_v + \not{D}_v^*] \\ G_v &= \frac{1+\not{v}}{2}[D_{0v}^* - iD_{1v}\gamma_5] \ . \end{aligned} \tag{2.25}$$

[1] The chiral field defined by Eq. (2.19) includes only scalar and iso-scalar meson (σ), and pseudo-scalar and iso-vector mesons (π^a), while the right-hand-side in Eq. (2.20) contains scalar and iso-vector meson (a_0^a), and pseudo-scalar and iso-scalar meson (η) in addition. σ meson and pions are, however, regarded as a chiral partner so that the transformation law in Eq. (2.20) is consistent.

By utilizing Eq. (2.24), the Lagrangian (2.18) is expressed in terms of H_v and G_v doublets as

$$\begin{aligned}
\mathcal{L}_{\rm HMET} &= \mathrm{tr}[G_v(iv\cdot\partial)\bar{G}_v] - \mathrm{tr}[H_v(iv\cdot\partial)\bar{H}_v] \\
&+ \frac{\Delta_m}{4f_\pi}\mathrm{tr}\big[G_v(M+M^\dagger)\bar{G}_v + H_v(M+M^\dagger)\bar{H}_v \\
&\quad -iG_v(M-M^\dagger)\gamma_5\bar{H}_v + iH_v(M-M^\dagger)\gamma_5\bar{G}_v\big] \\
&+ \frac{ig}{4f_\pi}\mathrm{tr}\big[G_v\gamma_5(\not\partial M^\dagger - \not\partial M)\bar{G}_v - H_v\gamma_5(\not\partial M^\dagger - \not\partial M)\bar{H}_v \\
&\quad -iG_v(\not\partial M^\dagger + \not\partial M)\bar{H}_v - iH_v(\not\partial M^\dagger + \not\partial M)\bar{G}_v\big]\ .
\end{aligned} \tag{2.26}$$

The effective Lagrangian in terms of D mesons are further derived by substituting (2.25). In this dissertation, however, I study $\bar{D}$ mesons in nuclear matter. The effective Lagrangian for $\bar{D}$ mesons are obtained by taking the charge conjugation. Then we find

$$\begin{aligned}
\mathcal{L}_{\rm HMET} &= 2\bar{D}_v(iv\cdot\partial)\bar{D}_v^\dagger - 2\bar{D}^*_{v,\mu}(iv\cdot\partial)\bar{D}_v^{*\dagger\mu} + 2\bar{D}^*_{0v}(iv\cdot\partial)\bar{D}_{0v}^{*\dagger} - 2\bar{D}_{1v,\mu}(iv\cdot\partial)\bar{D}_{1v}^{\dagger\mu} \\
&+ \frac{\Delta_m}{2f_\pi}\big[\bar{D}^*_{0v}(M+M^\dagger)\bar{D}_{0v}^{*\dagger} - \bar{D}_{1v,\mu}(M+M^\dagger)\bar{D}_{1v}^{\dagger\mu} \\
&\quad -\bar{D}_v(M+M^\dagger)\bar{D}_v^\dagger + \bar{D}^*_{v,\mu}(M+M^\dagger)\bar{D}_v^{*\dagger\mu}\big] \\
&+ \frac{\Delta_m}{2f_\pi}\big[\bar{D}^*_{0v}(M-M^\dagger)\bar{D}_v^\dagger - \bar{D}_{1v,\mu}(M-M^\dagger)\bar{D}_v^{*\dagger\mu} \\
&\quad -\bar{D}_v(M-M^\dagger)\bar{D}_{0v}^{*\dagger} + \bar{D}^{*\dagger}_{v,\mu}(M-M^\dagger)\bar{D}_{1v}^{\dagger\mu}\big] \\
&- \frac{g}{2f_\pi}\big[\bar{D}^\mu_{1v}(\partial_\mu M^\dagger - \partial_\mu M)\bar{D}_{0v}^{*\dagger} - \bar{D}^*_{0v}(\partial_\mu M^\dagger - \partial_\mu M)\bar{D}_{1v}^{\dagger\mu} \\
&\quad -\epsilon^{\mu\nu\rho\sigma}\bar{D}_{1v,\mu}(\partial_\nu M^\dagger - \partial_\nu M)\bar{D}^\dagger_{1v,\rho}v_\sigma\big] \\
&+ \frac{g}{2f_\pi}\big[\bar{D}^{*\mu}_v(\partial_\mu M^\dagger - \partial_\mu M)\bar{D}_v^\dagger - \bar{D}_v(\partial_\mu M^\dagger - \partial_\mu M)\bar{D}_v^{*\dagger\mu} \\
&\quad -\epsilon^{\mu\nu\rho\sigma}\bar{D}^*_{v,\mu}(\partial_\nu M^\dagger - \partial_\nu M)\bar{D}^{*\dagger}_{v,\rho}v_\sigma\big] \\
&+ \frac{g}{2f_\pi}[\bar{D}^\mu_{1v}(\partial_\mu M^\dagger + \partial_\mu M)\bar{D}_v^\dagger + \bar{D}_v(\partial_\mu M^\dagger + \partial_\mu M)\bar{D}_{1v}^{\dagger\mu}] \\
&- \frac{g}{2f_\pi}[\bar{D}^*_{0v}(\partial_\mu M^\dagger + \partial_\mu M)\bar{D}_v^{*\dagger\mu} + \bar{D}^{*\mu}_v(\partial_\mu M^\dagger + \partial_\mu M)\bar{D}_{0v}^{*\dagger}] \\
&- \frac{g}{2f_\pi}[\epsilon^{\mu\nu\rho\sigma}\bar{D}_{1v,\nu}(\partial_\rho M^\dagger + \partial_\rho M)\bar{D}^{*\dagger}_{v,\mu}v_\sigma + \epsilon^{\mu\nu\rho\sigma}\bar{D}^*_{v,\mu}(\partial_\rho M^\dagger + \partial_\rho M)\bar{D}^\dagger_{1v,\nu}v_\sigma]\ .
\end{aligned} \tag{2.27}$$

For later use, it is more convenient to further rewrite the Lagrangian (2.27) in a relativistic form. It is obtained by using $\bar{D} = \frac{1}{\sqrt{m}} \mathrm{e}^{-imv\cdot x} \bar{D}_v$ as

$$
\begin{aligned}
\mathcal{L} &= \partial_\mu \bar{D}_0^* \partial^\mu \bar{D}_0^{*\dagger} - m^2 \bar{D}_0^* \bar{D}_0^{*\dagger} - \partial_\mu \bar{D}_{1\nu} \partial^\mu \bar{D}_1^{\dagger\nu} + \partial_\mu \bar{D}_{1\nu} \partial^\nu \bar{D}_1^{\dagger\mu} + m^2 \bar{D}_{1\mu} \bar{D}_1^{\dagger\mu} \\
&+ \partial_\mu \bar{D} \partial^\mu \bar{D}^\dagger - m^2 \bar{D} \bar{D}^\dagger - \partial_\mu \bar{D}_\nu^* \partial^\mu \bar{D}^{*\dagger\nu} + \partial_\mu \bar{D}_\nu^* \partial^\nu \bar{D}^{*\dagger\mu} + m^2 \bar{D}_\mu^* \bar{D}^{*\dagger\mu} \\
&- \frac{1}{2} \frac{m\Delta_m}{f_\pi} [\bar{D}_0^* (M + M^\dagger) \bar{D}_0^{*\dagger} - \bar{D}_{1\mu} (M + M^\dagger) \bar{D}_1^{\dagger\mu} - \bar{D} (M + M^\dagger) \bar{D}^\dagger + \bar{D}_\mu^* (M + M^\dagger) \bar{D}^{*\mu\dagger}] \\
&- \frac{1}{2} \frac{m\Delta_m}{f_\pi} [\bar{D}_0^* (M - M^\dagger) \bar{D}^\dagger - \bar{D}_{1\mu} (M - M^\dagger) \bar{D}^{*\dagger\mu} - \bar{D} (M - M^\dagger) \bar{D}_0^{*\dagger} + \bar{D}_\mu^* (M - M^\dagger) \bar{D}_1^{\dagger\mu}] \\
&- \frac{g}{2} \frac{m}{f_\pi} [\bar{D}_1^\mu (\partial_\mu M^\dagger - \partial_\mu M) \bar{D}_0^{*\dagger} - \bar{D}_0^* (\partial_\mu M^\dagger - \partial_\mu M) \bar{D}_1^{\dagger\mu} - \frac{1}{m} \epsilon^{\mu\nu\rho\sigma} \bar{D}_{1\mu} (\partial_\nu M^\dagger - \partial_\nu M) i\partial_\sigma \bar{D}_{1\rho}^\dagger] \\
&+ \frac{g}{2} \frac{m}{f_\pi} [\bar{D}^{*\mu} (\partial_\mu M^\dagger - \partial_\mu M) \bar{D}^\dagger - \bar{D} (\partial_\mu M^\dagger - \partial_\mu M) \bar{D}^{*\dagger\mu} - \frac{1}{m} \epsilon^{\mu\nu\rho\sigma} \bar{D}_\mu^* (\partial_\nu M^\dagger - \partial_\nu M) i\partial_\sigma \bar{D}_\rho^{*\dagger}] \\
&+ \frac{g}{2} \frac{m}{f_\pi} [\bar{D}_1^\mu (\partial_\mu M^\dagger + \partial_\mu M) \bar{D}^\dagger + \bar{D} (\partial_\mu M^\dagger + \partial_\mu M) \bar{D}_1^{\dagger\mu}] \\
&- \frac{g}{2} \frac{m}{f_\pi} [\bar{D}_0^* (\partial_\mu M^\dagger + \partial_\mu M) \bar{D}^{*\dagger\mu} + \bar{D}^{*\mu} (\partial_\mu M^\dagger + \partial_\mu M) \bar{D}_0^{*\dagger}] \\
&- \frac{g}{2} \frac{1}{f_\pi} [\epsilon^{\mu\nu\rho\sigma} \bar{D}_{1\nu} (\partial_\rho M^\dagger + \partial_\rho M) i\partial_\sigma \bar{D}_\mu^{*\dagger} + \epsilon^{\mu\nu\rho\sigma} \bar{D}_\mu^* (\partial_\rho M^\dagger + \partial_\rho M) i\partial_\sigma \bar{D}_{1\nu}^\dagger] \ , \qquad (2.28)
\end{aligned}
$$

This Lagrangian is the fundamental Lagrangian for analysis which will be done in Chap. 4 and Chap. 5.

In the vacuum, chiral symmetry is spontaneously broken, which is expressed by taking the vacuum expectation value (VEV) of the chiral field as $\langle M \rangle_0 = f_\pi$ in the present model [2]. Therefore, the squared masses for $H_v = (\bar{D}, \bar{D}^*)$ mesons and the squared masses for $G_v = (\bar{D}_0^*, \bar{D}_1)$ mesons together with the spontaneous breakdown of chiral symmetry are read from Eq. (2.28) as

$$
\begin{aligned}
m_H^2 &= m^2 - m\Delta_m \qquad (2.29) \\
m_G^2 &= m^2 + m\Delta_m \ , \qquad (2.30)
\end{aligned}
$$

respectively. Then, using a hierarchy $m \gg \Delta_m$, we find following mass formulae

$$
\begin{aligned}
m &= m_G + m_H \qquad (2.31) \\
\Delta_m &= m_G - m_H \ . \qquad (2.32)
\end{aligned}
$$

[2]We have assumed that parity is not violated in QCD so that pions do not have their VEVs. Also, We have used a fact that the VEV of σ meson is identical to the pion decay constant f_π in the vacuum. In general, the mean field of σ meson can differ from f_π.

When we take m_H and m_G as a spin-averaged masses of $(\bar{D}, \bar{D}^*)$ and $(\bar{D}_0^*, \bar{D}_1)$ defined by

$$m_H = \frac{m_{\bar{D}} + 3m_{\bar{D}^*}}{4} \tag{2.33}$$

$$m_G = \frac{m_{\bar{D}_0^*} + 3m_{\bar{D}_1}}{4} , \tag{2.34}$$

respectively, and use the following observed values $m_{\bar{D}} = 1869$ MeV, $m_{\bar{D}^*} = 2010$ MeV, $m_{\bar{D}_0^*} = 2318$ MeV and $m_{\bar{D}_1} = 2427$ MeV, the parameters m and Δ_m are fixed as

$$m = 2190 \text{ MeV} \tag{2.35}$$

$$\Delta_m = 430 \text{ MeV} . \tag{2.36}$$

The other parameter g is determined by the decay width $\Gamma_{D^* \to D\pi}$ as $g = 0.50$.

Finally, let us make a comment on the chiral partner structure for $\bar{D}$ mesons. In obtaining the relations (2.29) and (2.30), we have taken the VEV of σ meson to be the pion decay constant f_π. When we access to an extreme environments such as temperature and density at which chiral symmetry is expected to be restored, the VEV of σ meson σ_0 is not identical to f_π. In this case, the masses of $H_v = (\bar{D}, \bar{D}^*)$ and $G_v = (\bar{D}_0^*, \bar{D}_1)$ are read as

$$m_H^* = m - \frac{G_\pi \sigma_0}{2} \tag{2.37}$$

$$m_G^* = m + \frac{G_\pi \sigma_0}{2} , \tag{2.38}$$

where we have defined $G_\pi = \Delta_m / f_\pi = 4.65$ for the convenience. These mass relations claim that the mass difference between $G_v = (\bar{D}_0^*, \bar{D}_1)$ and $H_v = (\bar{D}, \bar{D}^*)$ is of the form

$$\Delta_m^* \equiv m_G^* - m_H^* = G_\pi \sigma_0 . \tag{2.39}$$

Therefore, the mass difference between chiral partners is generated by the spontaneous breakdown of chiral symmetry since it is proportional to the VEV of σ meson. Particularly, the mass of chiral partners coincide at which chiral symmetry is completely restored: $m_G^* = m_H^*$ with $\sigma_0 = 0$.

Chapter 3

Linear sigma model in nuclear matter

In this chapter, I consider the linear sigma model and construct nuclear matter within this model. First, I review the linear sigma model and see how the spontaneous breakdown of chiral symmetry is demonstrated in Sec. 3.1. Next, in Sec. 3.2, I show the partial restoration of chiral symmetry in nuclear matter by employing the method of relativistic finite density field theory given in Appendix. A. Also, treatments of fluctuations of σ meson and pion respecting chiral symmetry are provided.

3.1 Linear sigma model

In this section, I review the linear sigma model [35, 36]. This model provides us with various aspects of chiral symmetry breakdown and related phenomena despite its simple appearance. This model will be utilized in calculations in Chap. 4 to describe the partial restoration of chiral symmetry in nuclear matter.

The conventional linear sigma model for two flavor is given by

$$\begin{aligned}\mathcal{L}_{\rm LS} &= \bar{\psi}_L i\partial\!\!\!/\psi_L + \bar{\psi}_R i\partial\!\!\!/\psi_R - g_Y\big(\bar{\psi}_L M\psi_R + \bar{\psi}_R M^\dagger\psi_L\big) \\ &\quad + \frac{1}{4}\mathrm{tr}\big[\partial_\mu M\partial^\mu M^\dagger\big] - \frac{m_0^2}{4}\mathrm{tr}\big[MM^\dagger\big] - \frac{\lambda}{16}\big(\mathrm{tr}\big[MM^\dagger\big]\big)^2 + \epsilon\sigma \ , \end{aligned} \tag{3.1}$$

where ψ_L and ψ_R are left-handed and right-handed two component nucleon fields, respectively, and M is the chiral field introduced in Eq (2.19). g_Y, m_0, λ and ϵ are free parameters. The transformation laws under the $SU(2)_L \times SU(2)_R$ chiral transformation for the nucleon ψ_L and ψ_R are

$$\psi_L \to g_L\psi_L \ , \quad \psi_R \to g_R\psi_R \ , \tag{3.2}$$

so that we find the Lagrangian (3.1) is chiral invariant except for the last term in the second line in Eq. (3.1) together with Eq. (2.21). This explicit chiral breaking term $\mathcal{L}_{\rm ex} = \epsilon\sigma$ is introduced to take into account the finite mass of pions. The linear sigma model in (3.1) is often rewritten in terms of ψ as

$$\begin{aligned}\mathcal{L}_{\rm LS} &= \bar{\psi} i\partial\!\!\!/ \psi - g_Y \bar{\psi} M_5 \psi \\ &\quad + \frac{1}{4}\mathrm{tr}\big[\partial_\mu M \partial^\mu M^\dagger\big] - \frac{m_0^2}{4}\mathrm{tr}\big[MM^\dagger\big] - \frac{\lambda}{16}\big(\mathrm{tr}\big[MM^\dagger\big]\big)^2 + \epsilon\sigma \ , \end{aligned} \tag{3.3}$$

where M_5 is defined by $M_5 = \sigma + i\gamma_5 \pi^a \tau^a$.

The spontaneous breakdown of chiral symmetry occurs when σ meson has its VEV since σ meson is not chiral singlet. This breakdown is triggered by an instability of the ground state realized when m_0^2 is negative. Then, by separating σ meson into the VEV and fluctuation as $\sigma \to \sigma_0 + \sigma$, the Lagrangian under the spontaneous breakdown of chiral symmetry is of the form

$$\begin{aligned}\mathcal{L}_{\rm LS} &= \bar{\psi} i\partial\!\!\!/ \psi - m_N \bar{\psi}\psi - g_Y \bar{\psi} M_5 \psi \\ &\quad + \frac{1}{2}\partial_\mu \sigma \partial^\mu \sigma - \frac{1}{2}(m_0^2 + 3\lambda\sigma_0^2)\sigma^2 + \frac{1}{2}\partial_\mu \pi^a \partial^\mu \pi^a - \frac{1}{2}(m_0^2 + \lambda\sigma_0^2)\pi^a\pi^a \\ &\quad + (\text{interactions}) \ . \end{aligned} \tag{3.4}$$

m_N is defined by $m_N = g_Y \sigma_0$ and this quantity is regarded as the mass of nucleon. (interactions) in the third line in Eq. (3.4) collectively denotes the interaction terms among σ meson and pion. In order to take account that σ_0 represents the true vacuum, we need to solve a gap equation. This equation actually ensures that one point function (tadpole diagram) of σ meson vanishes. The gap equation is derived as

$$m_0^2 \sigma_0 + \lambda \sigma_0^3 = \epsilon \ . \tag{3.5}$$

In Eq. (3.4), I have demonstrated that the nucleon mass is dynamically generated by the spontaneous breakdown of chiral symmetry in a simple way. Note the Lagrangian in Eq. (3.4) together with the gap equation in Eq. (3.5) tells us that the mass of pion is read as $m_\pi^2 = \frac{\epsilon}{\sigma_0}$. Namely, the pion mass vanishes when the original $SU(2)_L \times SU(2)_R$ chiral symmetry is exact. This indicates pion is the Nambu-Goldstone boson (NG boson). As I have mentioned in Sec. 2.3, the VEV of σ meson σ_0 is identical to the pion decay constant f_π in the vacuum.

3.2 Partial restoration of chiral symmetry in nuclear matter

Here, I demonstrate how the partial restoration of chiral symmetry in nuclear matter occurs in the linear sigma model.

In this study, nuclear matter is constructed by a nucleon one-loop. From the Lagrangian in Eq. (3.4), the effective action with nucleon one-loop and the homogeneous VEV of σ meson is obtained by performing the path integral with respect to the nucleon field as

$$\begin{aligned}\Gamma[\sigma,\pi;\sigma_0] &= -i\mathrm{Tr}\ln(i\partial\!\!\!/ + \mu_B\gamma^0 - g_Y(\sigma_0+\sigma+i\gamma_5\tau^a\pi^a)) \\ &+ \int d^4x\Big(\frac{1}{2}\partial_\mu\sigma\partial^\mu\sigma + \frac{1}{2}\partial_\mu\pi^a\partial^\mu\pi^a - \frac{m_0^2}{2}((\sigma_0+\sigma)^2+\pi^2) \\ &\quad -\frac{\lambda}{4}((\sigma_0+\sigma)^2+\pi^2)^2 + \epsilon(\sigma_0+\sigma)\Big)\ ,\end{aligned} \tag{3.6}$$

where we have added a baryon number chemical potential μ_B to take the baryon number density into account. "Tr" in Eq. (3.6) represents the trace for spin, isospin and space-time coordinate. The gap equation is derived by taking a derivative with respect to σ_0 with $\sigma=\pi=0$ as

$$\frac{\partial\Gamma[0,0;\sigma_0]}{\partial\sigma_0} = TV\left(2g_Y\mathrm{tr}\int\frac{\tilde{d}^4k}{(2\pi)^4}\tilde{G}_N(k) - m_0^2\sigma_0 - \lambda\sigma_0^3 + \epsilon\right) = 0\ . \tag{3.7}$$

TV is the infinite volume of space-time. The factor 2 in Eq. (3.7) appears due to the isospin degrees of freedom. In Eq. (3.7), we have defined the in-medium propagator of the nucleon by $\tilde{G}_N(k)$ derived in Eq. (A.9) which takes the form of

$$\tilde{G}_N(k_0,\vec{k}) = (k\!\!\!/ + m_N)\left[\frac{i}{k^2-m_N^2+i\epsilon} - 2\pi\theta(k_0)\theta(k_F-|\vec{k}|)\delta(k^2-m_N^2)\right]\ , \tag{3.8}$$

where we have defined $m_N = g_Y\sigma_0$. $\theta(x)$ is the Heaviside's step function and $\delta(x)$ is the Dirac's delta function. k_F is the Fermi momentum which is defined in terms of the chemical potential by $\mu_B = \sqrt{k_F^2+m_N^2}$, and is related to the baryon number density ρ_B by

$$\rho_B = \frac{2}{3\pi^2}k_F^3\ . \tag{3.9}$$

In the present analysis, I only pick up the density dependent part of the integral since our present study is intended to investigate the partial restoration of chiral symmetry in nuclear matter. Then, the symbol $\tilde{d}^4k$ in the first line in Eq. (3.7) indicates a momentum integral for density dependent part. Namely, if we define a function $F(k_0, \vec{k}; k_F)$ with k_F being the Fermi momentum, the integral $\tilde{d}^4k$ refers to

$$\int \frac{\tilde{d}^4k}{(2\pi)^4} F(k_0, \vec{k}; k_F) \equiv \int \frac{d^4k}{(2\pi)^4} F(k_0, \vec{k}; k_F) - \int \frac{d^4k}{(2\pi)^4} F(k_0, \vec{k}; k_F = 0) \ . \quad (3.10)$$

Therefore, the gap equation in Eq. (3.7) is explicitly reduced to

$$-4g_Y \int \frac{d^3k}{(2\pi)^3} \frac{m_N}{\sqrt{|\vec{k}|^2 + m_N^2}} = m_0^2\sigma_0^2 + \lambda\sigma_0^3 - \epsilon \ . \quad (3.11)$$

By inserting the gap equation in Eq. (3.11) so as to cancel the one-point function of σ meson, the effective action is expanded up to the quadratic terms with respect to σ and pion as

$$\begin{aligned}
\Gamma[\sigma, \pi; \sigma_0] &= -i\mathrm{Tr}\ln(i\partial\!\!\!/ - m_N + \mu_B\gamma^0) \\
&+ i\frac{g^2}{2}\mathrm{Tr}\left[\frac{1}{i\partial\!\!\!/ - m_N + \mu_B\gamma^0}\sigma\frac{1}{i\partial\!\!\!/ - m_N + \mu_B\gamma^0}\sigma\right] \\
&+ i\frac{g^2}{2}\mathrm{Tr}\left[\frac{1}{i\partial\!\!\!/ - m_N + \mu_B\gamma^0}i\gamma_5\pi^a\tau^a\frac{1}{i\partial\!\!\!/ - m_N + \mu_B\gamma^0}i\gamma_5\pi^b\tau^b\right] \\
&+ \int d^4x \left\{\frac{1}{2}\partial_\mu\sigma\partial^\mu\sigma + \frac{1}{2}\partial_\mu\pi^a\partial^\mu\pi^a - \frac{1}{2}(m_0^2 + 3\lambda\sigma_0^2)\sigma^2 - \frac{1}{2}(m_0^2 + \lambda\sigma_0^2)\pi^a\pi^a\right\} \\
&+ \cdots \ .
\end{aligned} \quad (3.12)$$

From this form, we easily find the propagators of σ meson and pion around the new ground state determined by the gap equation in Eq. (3.11). They are defined by the inverse of second functional derivative as

$$\begin{aligned}
i\tilde{G}_\sigma^{-1}(q_0, \vec{q}) &\equiv \mathrm{F.T.}\ \frac{\delta^2\Gamma[\sigma, \pi; \sigma_0]}{\delta\sigma(x)\delta\sigma(y)} \\
&= q^2 - (m_0^2 + 3\lambda\sigma_0^2) - 2ig^2\int \frac{\tilde{d}^4k}{(2\pi)^4}\mathrm{tr}\left[\tilde{G}_N(k_0, \vec{k})\tilde{G}_N(k_0 - q_0, \vec{k} - \vec{q})\right] \\
&\equiv q^2 - m_\sigma^2 - i\tilde{\Sigma}_\sigma(q_0, \vec{q}) \ ,
\end{aligned} \quad (3.13)$$

and

$$
\begin{aligned}
i\tilde{G}_{\pi}^{ab,-1}(q_0,\vec{q}) &\equiv \text{F.T.}\ \frac{\delta^2\Gamma[\sigma,\pi;\sigma_0]}{\delta\pi^a(x)\delta\pi^b(y)} \\
&= \left(q^2-(m_0^2+\lambda\sigma_0^2)-2ig^2\int\frac{\tilde{d}^4k}{(2\pi)^4}\mathrm{tr}\left[i\gamma_5\tilde{G}_N(k_0,\vec{k})i\gamma_5\tilde{G}_N(k_0-q_0,\vec{k}-\vec{q})\right]\right)\delta^{ab} \\
&\equiv \left(q^2-m_\pi^2-i\tilde{\Sigma}_\pi(q_0,\vec{q})\right)\delta^{ab}\ . \qquad (3.14)
\end{aligned}
$$

The symbol "F.T." in Eqs (3.13) and (3.14) represents the Fourier transformation.

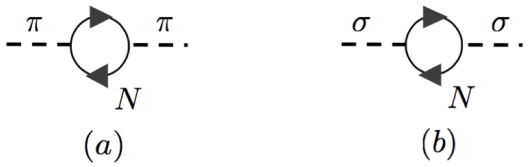

Figure 3.1: Self-energies for (a) pion $\tilde{\Sigma}_\pi(q_0,\vec{q})$ and (b) σ meson $\tilde{\Sigma}_\sigma(q_0,\vec{q})$.

The diagrammatic picture of self-energies for pion and σ meson denoted by $\tilde{\Sigma}_\pi(q_0,\vec{q})$ and $\tilde{\Sigma}_\sigma(q_0,\vec{q})$ are shown in Fig. 3.1. I should note that it is obvious these propagators

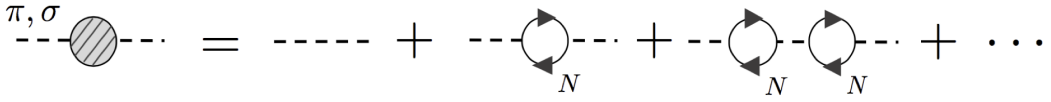

Figure 3.2: Propagators for pion and σ meson should include infinite sums of nucleon one-loops to preserve chiral symmetry.

are fully respecting the original chiral symmetry since they are derived from the effective action directly. Furthermore, they should include infinite sums of nucleon loops as indicated in Fig. 3.2.

Finally, we put some physical values into the parameters and solve the gap equation in Eq. (3.11) numerically. Here, we use pion mass $m_\pi = 138$ MeV, nucleon mass $m_N = 939$ MeV, pion decay constant $f_\pi = 92.4$ MeV and sigma term $\Sigma_{\pi N} = 45$ MeV

as inputs. Then, from the relations [1]

$$\begin{aligned} m_N &= g f_\pi, \\ \Sigma_{\pi N} &= g \frac{f_\pi^2 m_\pi^2}{2\lambda f_\pi^3 + \epsilon}, \\ m_0^2 + \lambda f_\pi^2 &= \frac{\epsilon}{f_\pi}, \\ m_\pi^2 &= \frac{\epsilon}{f_\pi}, \end{aligned} \tag{3.16}$$

the parameters g_Y, λ, m_0^2 and ϵ are fixed as

$$\begin{aligned} g_Y &= 10.2, \\ \lambda &= 22.2, \\ m_0^2 &= -1.70 \times 10^5 \text{ MeV}^2, \\ \epsilon &= 1.76 \times 10^6 \text{ MeV}^3. \end{aligned} \tag{3.17}$$

These values allow us to solve the gap equation in Eq. (3.11) numerically, and the

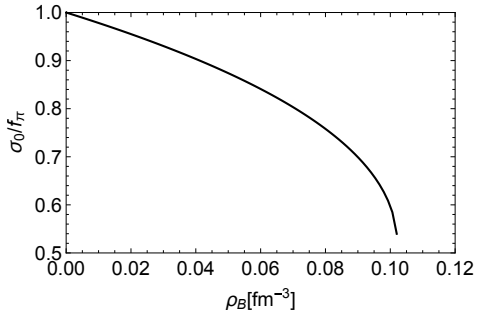

Figure 3.3: Density dependence of the mean field σ_0.

resultant density dependence of σ_0 is plotted in Fig. 3.3. As indicated in this figure, the VEV of σ meson decreases as the baryon number density increases. This tendency explicitly shows the partial restoration of chiral symmetry in nuclear matter. Note

[1] The sigma term $\Sigma_{\pi N}$ is defined in association with a slope of σ_0 by

$$\Sigma_{\pi N} \equiv -f_\pi m_\pi^2 \frac{\partial \sigma_0}{\partial \rho_B}\Big|_{\rho_B = 0} . \tag{3.15}$$

The formula in the second line in Eq. (3.16) is derived by taking a derivative in Eq. (3.11) with respect to ρ_B and setting $\rho_B = 0$ together with Eq. (3.15).

that the tendency of restoration is observed only at $\rho_B \lesssim 0.10$ fm^{-3}, which is lower than the normal nuclear matter density $\rho_B^* \approx 0.16$ fm^{-3} [41]. In the present analysis, however, I investigate the qualitative tendency of modifications of $\bar{D}$ mesons at low density regime. Therefore, I utilize this linear sigma model to describe nuclear matter for calculations of $\bar{D}$ mesons in Chap. 4.

Chapter 4

Modifications of $\bar{D}$ mesons in nuclear matter

Here, I study the modifications of $\bar{D}$ mesons in nuclear matter by employing the effective Lagrangian for $\bar{D}$ mesons based on the chiral partner structure derived in Chap. 2 and the linear sigma model introduced in Chap. 3 to describe the medium. In the context of the chiral partner structure, the mass difference between positive-parity meson and negative-parity meson are related to the spontaneous breakdown of chiral symmetry as shown in Sec. 2.3. Therefore, I particularly focus on $\bar{D}$ (0^-) meson and $\bar{D}_0^*$ (0^+) meson in this chapter. First, I investigate masses of these $\bar{D}$ mesons in nuclear matter by taking into account mean field σ_0, Hartree-type and Fock-type one-loop contributions in Sec.4.1. In Sec. 4.2, spectral functions for $\bar{D}$ mesons are studied so as to find vestiges of the changes of chiral symmetry in nuclear matter.

4.1 Masses of $\bar{D}$ and $\bar{D}_0^*$ meson in nuclear matter

In this section, I study masses of $\bar{D}$ and $\bar{D}_0^*$ mesons. From the Lagrangian in Eq. (2.28) based on the chiral partner structure, masses of $\bar{D}$ mesons are derived as in Eqs. (2.37) and (2.38), where m_H^* and m_G^* indicate the spin-averaged masses of $(\bar{D}, \bar{D}^*)$ mesons and $(\bar{D}_0^*, \bar{D}_1)$ mesons, respectively. In these equations, σ_0 is the mean field of σ meson (the VEV of σ meson) which is not identical to the pion decay constant f_π since we suppose nuclear matter. The values of parameters m and Δ_m are given by Eqs. (2.35) and (2.36), respectively. The analysis in Sec. 2.3 have done under the HQSS. In the real world, however, this symmetry is slightly violated since the mass of a charm quark does not diverge as mentioned in Sec. 2.2. Therefore, we

need to include such violation to make our discussion more realistic. This effect is incorporated by changing mass formulae as

$$\begin{aligned} m_{\bar{D}} &= m - \frac{G_\pi \sigma_0}{2} - \frac{\Delta_{\bar{D}}}{2} , \\ m_{\bar{D}^*} &= m - \frac{G_\pi \sigma_0}{2} + \frac{\Delta_{\bar{D}^*}}{2} , \\ m_{\bar{D}_0^*} &= m + \frac{G_\pi \sigma_0}{2} - \frac{\Delta_{\bar{D}_0^*}}{2} , \\ m_{\bar{D}_1} &= m + \frac{G_\pi \sigma_0}{2} + \frac{\Delta_{\bar{D}_1}}{2} , \end{aligned} \tag{4.1}$$

where $\Delta_{\bar{D}}$, $\Delta_{\bar{D}^*}$, $\Delta_{\bar{D}_0^*}$ and $\Delta_{\bar{D}_1}$ are given so as to reproduce the masses of $\bar{D}$, $\bar{D}^*$, $\bar{D}_0^*$ and $\bar{D}_1$ mesons in the vacuum: $m_{\bar{D}} = 1869$ MeV, $m_{\bar{D}^*} = 2010$ MeV, $m_{\bar{D}_0^*} = 2318$ MeV and $m_{\bar{D}_1} = 2427$ MeV. Then, these are fixed as $\Delta_{\bar{D}} = 202$ MeV, $\Delta_{\bar{D}^*} = 80$ MeV, $\Delta_{\bar{D}_0^*} = 164$ MeV and $\Delta_{\bar{D}_1} = 54$ MeV by using a fact of $\sigma_0 = f_\pi$ in the vacuum.

The mean field of σ meson is expected to be changed by including one-loop diagrams of σ meson and pion as $\sigma_0 \to \sigma_0 + \delta\sigma_0$ (δ_0 represents the one-loop correction), since $\sigma\sigma\sigma$ vertex and $\sigma\pi\pi$ vertex are derived in the linear sigma model. In calculating these one-loop diagrams, we must utilize the propagators of σ meson and pion obtained in Eqs. (3.13) and (3.14) or diagrammatically shown in Fig. 3.2, in order to respect chiral symmetry as explained in Sec. 3.2. By keeping in mind this treatment, the one-loop corrections to the mean field $\delta\sigma_0$ are included as

$$\begin{aligned} \delta\sigma_0 &= -\frac{3\lambda\sigma_0}{\tilde{m}_\sigma^2} \int \frac{d^4k}{(2\pi)^4} \Big(F(\vec{k};\Lambda)\Big)^2 \Big(\tilde{G}_\sigma(k_0,\vec{k}) - \tilde{G}_\sigma^{\rm vac}(k_0,\vec{k})\Big) \\ &\quad -\frac{3\lambda\sigma_0}{\tilde{m}_\sigma^2} \int \frac{d^4k}{(2\pi)^4} \Big(F(\vec{k};\Lambda)\Big)^2 \Big(\tilde{G}_\pi(k_0,\vec{k}) - \tilde{G}_\pi^{\rm vac}(k_0,\vec{k})\Big) \\ &= \frac{3\lambda\sigma_0}{\tilde{m}_\sigma^2} \int \frac{d^4k}{(2\pi)^4} \Big(F(\vec{k};\Lambda)\Big)^2 {\rm Im} \left[\frac{1}{k^2 - m_\sigma^2 - i\tilde{\Sigma}_\sigma(k_0,\vec{k})} - \frac{1}{k^2 - m_{\sigma,{\rm vac}}^2 + i\epsilon}\right] \\ &\quad +\frac{3\lambda\sigma_0}{\tilde{m}_\sigma^2} \int \frac{d^4k}{(2\pi)^4} \Big(F(\vec{k};\Lambda)\Big)^2 {\rm Im} \left[\frac{1}{k^2 - m_\pi^2 - i\tilde{\Sigma}_\pi(k_0,\vec{k})} - \frac{1}{k^2 - m_{\pi,{\rm vac}}^2 + i\epsilon}\right] \\ &= -\frac{3\lambda\sigma_0}{2\tilde{m}_\sigma^2} \int \frac{d^4k}{(2\pi)^4} \Big(F(\vec{k};\Lambda)\Big)^2 \epsilon(k_0) \Big\{\rho_\sigma(k_0,\vec{k}) - \rho_\sigma^{\rm vac}(k)\Big\} \\ &\quad -\frac{3\lambda\sigma_0}{2\tilde{m}_\sigma^2} \int \frac{d^4k}{(2\pi)^4} \Big(F(\vec{k};\Lambda)\Big)^2 \epsilon(k_0) \Big\{\rho_\pi(k_0,\vec{k}) - \rho_\pi^{\rm vac}(k_0,\vec{k})\Big\} \ . \end{aligned} \tag{4.2}$$

These are diagrammatically shown in Fig. 4.1. In Eq. (4.2), we have defined $\tilde{G}_\pi(k_0, \vec{k})$

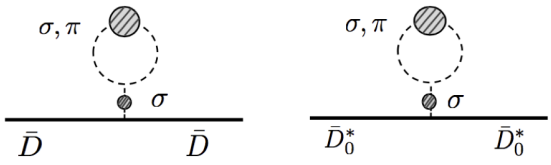

Figure 4.1: Hartree-type one-loop corrections ($\delta\sigma_0^*$) to the self-energies of $\bar{D}$ and $\bar{D}_0^*$ mesons. The meaning of blobs in these diagrams is provided in Fig. 3.2.

via by the following relation: $\tilde{G}_\pi^{ab}(k_0, \vec{k}) = \delta^{ab}\tilde{G}_\pi(k_0, \vec{k})$. $\tilde{G}_\sigma^{\rm vac}(k_0, \vec{k})$ and $\tilde{G}_\pi^{\rm vac}(k_0, \vec{k})$ are the propagators of σ meson and pion in the vacuum:

$$\begin{aligned} \tilde{G}_\pi^{\rm vac}(k_0, \vec{k}) &= \frac{i}{k^2 - m_{\sigma,\rm vac}^2 + i\epsilon} \\ \tilde{G}_\pi^{\rm vac}(k_0, \vec{k}) &= \frac{i}{k^2 - m_{\pi,\rm vac}^2 + i\epsilon} \ , \end{aligned} \tag{4.3}$$

where $m_{\sigma,\rm vac}$ and $m_{\pi,\rm vac}$ are the masses of σ meson and pion in the vacuum, respectively. $\tilde{m}_\sigma$ is the mass of σ meson in nuclear matter, i.e., this is defined by the energy at which $\tilde{G}_\sigma^{-1}(k_0, \vec{0}) = 0$ is satisfied. $F(\vec{k}, \Lambda)$ is the form factor to take hadronic size into account which is of the form

$$F(\vec{k}; \Lambda) = \frac{\Lambda^2}{|\vec{k}|^2 + \Lambda^2} \ , \tag{4.4}$$

where Λ is the cutoff parameter. In the present analysis, the value of Λ is fixed as $\Lambda = 300$ MeV, which is slightly higher than the Fermi momentum of the normal nuclear matter density. $\epsilon(k_0)$ in the last line in Eq. (4.2) is the sign function which is defined by $\epsilon(k_0) = +1$ for $k_0 > 0$ and $\epsilon(k_0) = -1$ for $k_0 < 0$. $\rho_{\sigma(\pi)}(k_0, \vec{k})$ is the spectral function for σ meson (pion) in nuclear matter calculated by using a useful relation in Eq. (A.20) as

$$\rho_{\sigma(\pi)}(k_0, \vec{k}) = \frac{-2{\rm Im}\tilde{\Sigma}_{\pi(\sigma)}^R(k_0, \vec{k})}{\left[k^2 - m_{\pi(\sigma)}^2 - {\rm Re}\tilde{\Sigma}_{\pi(\sigma)}^R(k_0, \vec{k})\right]^2 + \left[{\rm Im}\tilde{\Sigma}_{\pi(\sigma)}^R(k_0, \vec{k})\right]^2}, \tag{4.5}$$

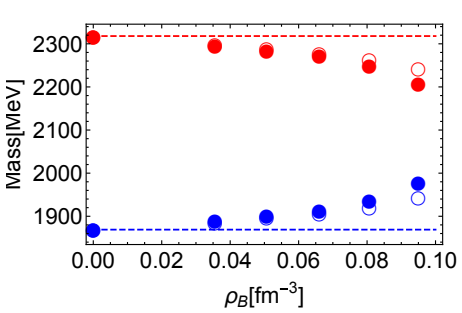

(a) Masses of $\bar{D}$ and $\bar{D}_0^*$ mesons.

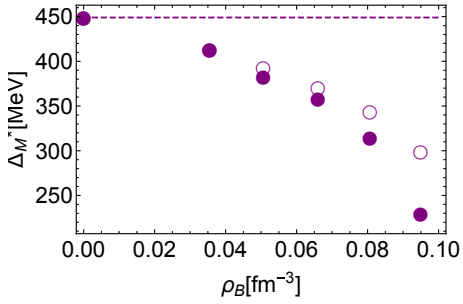

(b) Mass difference between $\bar{D}_0^*$ and $\bar{D}$ mesons.

Figure 4.2: (color online) The density dependence of (a) masses of $\bar{D}$ and $\bar{D}_0^*$ mesons and (b) that of mass difference between $\bar{D}_0^*$ and $\bar{D}$ mesons. The red filled circles and the blue filled circles in (a) denote the masses of $\bar{D}_0^*$ meson and $\bar{D}$, respectively, with Hartree-type one-loop corrections as well as the mean field. The open circles in (a) represent the results with mean field alone. In a similar way, the filled purple circles in (b) denote the mass difference between $\bar{D}_0^*$ and $\bar{D}$ mesons with mean field and Hartree-type one-loop corrections, while the open ones denote that with mean field alone. The dashed horizontal line corresponds to the vacuum values of them put as references.

where the symbol "R" refers to the retarded self-energy, and $\rho^{\rm vac}_{\sigma(\pi)}(k_0, \vec{k})$ is that in the vacuum

$$\rho^{\rm vac}_{\sigma(\pi)} = 2\pi\epsilon(k_0)\delta(k^2 - m^2_{\sigma(\pi),{\rm vac}}) \ . \tag{4.6}$$

The detail on the definition and derivation for them is given in Appendix A.

First, I show the density dependence of the masses of $\bar{D}$ and $\bar{D}_0^*$ mesons with Hartree-type one-loop corrections as well as the mean field. The resultant plot is indicated in Fig. 4.2. The red filled circles and the blue filled circles in Fig. 4.2 (a) denote the masses of $\bar{D}_0^*$ meson and $\bar{D}$ meson, respectively, with mean field and Hartree-type one-loop corrections. The open circles in Fig. 4.2 (a) represent the results with mean field alone. As we can see from this figure, the mass of $\bar{D}$ meson increases while that of $\bar{D}_0^*$ meson decreases as we can access to higher density. This tendency reflects the feature of chiral partner, i.e., mass difference between the partners is generated by the spontaneous breakdown of chiral symmetry and it is expected to get small as the density increases together with the partial restoration of chiral symmetry. To observe this change more clearly, I plot the density dependence

of the mass difference between $\bar{D}_0^*$ and $\bar{D}$ mesons in Fig. 4.2 (b). The filled purple circles in Fig. 4.2 (b) denote the mass difference between $\bar{D}_0^*$ and $\bar{D}$ mesons with Hartree-type one-loop corrections as well as the mean field, while the open ones denote that with mean field alone. I should note that mean field contributions are dominant and Hartree-type one-loop corrections are rather suppressed.

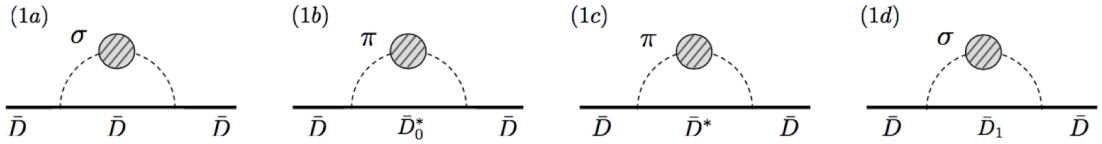

Figure 4.3: Fock-type one-loop corrections to the self-energy for $\bar{D}$ meson.

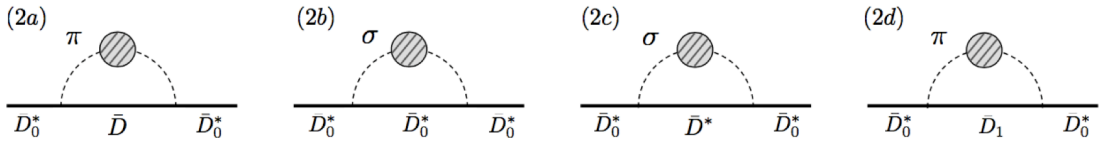

Figure 4.4: Fock-type one-loop corrections to the self-energy for $\bar{D}_0^*$ meson.

Next, I include Fock-type one loop corrections in addition to the Hartree-type one-loop corrections and the mean field which are diagrammatically indicated in Fig. 4.3 and Fig. 4.4. Again, the propagators of σ meson and pion in these figures must include infinite sums of nucleon loops as in Fig. 3.2. Calculations of these diagrams are complicated, so that, here, let us show the detailed calculation of the self-energy in Fig. 4.3 (1a) as an example. According to the arguments on finite density field theory [42] in Appendix A, the imaginary part of the retarded self-energy in Fig. 4.3 (1a) $\mathrm{Im}\tilde{\Sigma}^R_{\bar{D}(1a)}(q_0,\vec{q})$ is related to the greater self-energy $\tilde{\Sigma}^>_{\bar{D}(1a)}(q_0,\vec{q})$ and the lesser self-energy $\tilde{\Sigma}^<_{\bar{D}(1a)}(q_0,\vec{q})$ as

$$\mathrm{Im}\tilde{\Sigma}^R_{\bar{D}(1a)}(q_0,\vec{q}) = \frac{1}{2}\left(\tilde{\Sigma}^>_{\bar{D}(1a)}(q_0,\vec{q}) - \tilde{\Sigma}^<_{\bar{D}(1a)}(q_0,\vec{q})\right) \ . \tag{4.7}$$

This relation is shown in Eq (A.21). The real part of the retarded self-energy $\mathrm{Re}\tilde{\Sigma}^R_{\bar{D}(1a)}(q_0,\vec{q})$ is obtained via the subtracted dispersion relation derived in Eq. (A.25) as

$$\mathrm{Re}\tilde{\Sigma}^R_{\bar{D}(1a)}(q_0,\vec{q}) \ = \ \frac{q^2-m_{\bar{D}}^2}{\pi}\,\mathrm{P}\!\int_0^\infty dz^2 \frac{\mathrm{Im}\tilde{\Sigma}^R_{\bar{D}}(z,\vec{q})}{(z^2-q_0^2)(z^2-|\vec{q}|^2-m_{\bar{D}}^2)} \ , \tag{4.8}$$

where the symbol "P" stands for the principal value integral. Therefore, we need to compute the imaginary part of the retarded self-energy (4.7), namely, we firstly need to know the explicit forms of $\tilde{\Sigma}^{>}_{\bar{D}(1a)}(q_0,\vec{q})$ and $\tilde{\Sigma}^{<}_{\bar{D}(1a)}(q_0,\vec{q})$.

The greater and lesser self-energy in the coordinate space $\tilde{\Sigma}^{>}_{\bar{D}(1a)}(x_0,\vec{x})$ and $\tilde{\Sigma}^{<}_{\bar{D}(1a)}(x_0,\vec{x})$ are defined through $\Sigma_{\bar{D}(1a)}(x_0,\vec{x})$ by

$$\Sigma_{\bar{D}(1a)}(x_0,\vec{x}) = \theta(x_0)\Sigma^{>}_{\bar{D}(1a)}(x_0,\vec{x}) + \theta(-x_0)\Sigma^{<}_{\bar{D}(1a)}(x_0,\vec{x}) \ . \tag{4.9}$$

$\tilde{\Sigma}^{>}_{\bar{D}(1a)}(q_0,\vec{q})$ and $\tilde{\Sigma}^{<}_{\bar{D}(1a)}(q_0,\vec{q})$ are defined by the Fourier transformation of them. In a similar manner, the propagator of σ meson ($\bar{D}$ meson) is also decomposed into the greater part $G^{>}_{\sigma}(x_0,\vec{x})$ ($G^{>}_{\bar{D}}(x_0,\vec{x})$) and the lesser part $G^{<}_{\sigma}(x_0,\vec{x})$ ($G^{<}_{\bar{D}}(x_0,\vec{x})$) as

$$\begin{aligned} G_{\sigma}(x_0,\vec{x}) &= \theta(x_0)G^{>}_{\sigma}(x_0,\vec{x}) + \theta(-x_0)G^{<}_{\sigma}(x_0,\vec{x}) & (4.10)\\ G_{\bar{D}}(x_0,\vec{x}) &= \theta(x_0)G^{>}_{\bar{D}}(x_0,\vec{x}) + \theta(-x_0)G^{<}_{\bar{D}}(x_0,\vec{x}) & (4.11) \end{aligned}$$

in the coordinate space. Then, the self-energy in Fig. 4.3 (1a) $\Sigma_{\bar{D}(1a)}(x_0,\vec{x})$ is computed as

$$\begin{aligned} \Sigma_{\bar{D}(1a)}(x_0,\vec{x}) &= (imG_{\pi})^2\, G_{\bar{D}}(x_0,\vec{x})G_{\sigma}(x_0,\vec{x}) \\ &= (imG_{\pi})^2 \left[\theta(x_0)G^{>}_{\bar{D}}(x_0,\vec{x}) + \theta(-x_0)G^{<}_{\bar{D}}(x_0,\vec{x})\right] \\ &\quad \times \ \left[\theta(x_0)G^{>}_{\sigma}(x_0,\vec{x}) + \theta(-x_0)G^{<}_{\sigma}(x_0,\vec{x})\right] \\ &= (imG_{\pi})^2 \left[\theta(x_0)G^{>}_{\bar{D}}(x_0,\vec{x})G^{>}_{\sigma}(x_0,\vec{x}) + \theta(-x_0)G^{<}_{\bar{D}}(x_0,\vec{x})G^{<}_{\sigma}(x_0,\vec{x})\right] \ . \end{aligned} \tag{4.12}$$

This equation tells us $\tilde{\Sigma}^{>}_{\bar{D}(1a)}(x_0,\vec{x})$ and $\tilde{\Sigma}^{<}_{\bar{D}(1a)}(x_0,\vec{x})$ are expressed as

$$\begin{aligned} \Sigma^{>}_{\bar{D}(1a)}(x_0,\vec{x}) &= (imG_{\pi})^2\, G^{>}_{\bar{D}}(x_0,\vec{x})G^{>}_{\sigma}(x_0,\vec{x}) \\ \Sigma^{<}_{\bar{D}(1a)}(x_0,\vec{x}) &= (imG_{\pi})^2\, G^{<}_{\bar{D}}(x_0,\vec{x})G^{<}_{\sigma}(x_0,\vec{x}) \ , \end{aligned} \tag{4.13}$$

and the Fourier transformations of them leads to

$$\begin{aligned} \tilde{\Sigma}^{>}_{\bar{D}(1a)}(q_0,\vec{q}) &= (imG_{\pi})^2 \int \frac{d^4k}{(2\pi)^4} \left(F(\vec{k};\Lambda)\right)^2 \tilde{G}^{>}_{\bar{D}}(k_0,\vec{k})\tilde{G}^{>}_{\sigma}(q_0-k_0,\vec{q}-\vec{k}) \\ \tilde{\Sigma}^{<}_{\bar{D}(1a)}(q_0,\vec{q}) &= (imG_{\pi})^2 \int \frac{d^4k}{(2\pi)^4} \left(F(\vec{k};\Lambda)\right)^2 \tilde{G}^{<}_{\bar{D}}(k_0,\vec{k})\tilde{G}^{<}_{\sigma}(q_0-k_0,\vec{q}-\vec{k}) \ . \end{aligned} \tag{4.14}$$

In Eq. (4.14), we have again inserted the form factor $F(\vec{k},\Lambda)$ defined by Eq. (4.4), and $\tilde{G}^{>}_{\bar{D}(\sigma)}(k_0,\vec{k})$ and $\tilde{G}^{<}_{\bar{D}(\sigma)}(k_0,\vec{k})$ are the Fourier transformation of $\tilde{G}^{>}_{\bar{D}(\sigma)}(x_0,\vec{x})$

and $\tilde{G}^{<}_{\bar{D}(\sigma)}(x_0,\vec{x})$, respectively. From Eq. (A.33), we find that $\tilde{G}^{>}_{\bar{D}}(q_0,\vec{q})$, $\tilde{G}^{>}_{\sigma}(q_0,\vec{q})$, $\tilde{G}^{<}_{\bar{D}}(q_0,\vec{q})$ and $\tilde{G}^{<}_{\sigma}(q_0,\vec{q})$ take the forms of

$$\begin{aligned}
\tilde{G}^{>}_{\bar{D}}(q_0,\vec{q}) &= \theta(q_0)\rho_{\bar{D}}(q_0,\vec{q}) \quad , \quad \tilde{G}^{>}_{\sigma}(q_0,\vec{q}) = \theta(q_0)\rho_{\sigma}(q_0,\vec{q}) \ , \\
\tilde{G}^{<}_{\bar{D}}(q_0,\vec{q}) &= -\theta(-q_0)\rho_{\bar{D}}(q_0,\vec{q}) \quad , \quad \tilde{G}^{<}_{\sigma}(q_0,\vec{q}) = -\theta(q_0)\rho_{\sigma}(q_0,\vec{q}) \ ,
\end{aligned} \tag{4.15}$$

where $\rho_{\bar{D}}(q_0,\vec{q})$ is the spectral function of $\bar{D}$ meson at the mean field level as

$$\rho_{\bar{D}}(q_0,\vec{q}) = 2\pi\epsilon(q_0)\delta(q^2 - m^2_{\bar{D}}) \tag{4.16}$$

($m_{\bar{D}}$ is given in Eq. (4.1)), and $\rho_{\sigma}(q_0,\vec{q})$ is that of σ meson in nuclear matter obtained in Eq. (4.5). By substituting Eq. (4.14) into Eq. (4.7) together with relations in Eq. (4.15), we can find

$$\begin{aligned}
& \mathrm{Im}\tilde{\Sigma}^{R}_{\bar{D}(1a)}(q_0,\vec{q}) \\
= \ & \frac{1}{2}\left(\tilde{\Sigma}_{\bar{D}(1a)}(q_0,\vec{q}) - \tilde{\Sigma}^{<}_{\bar{D}(1a)}(q_0,\vec{q})\right) \\
= \ & \frac{1}{2}\left(imG_\pi\right)^2 \int \frac{d^4k}{(2\pi)^4}\left(F(\vec{k};\Lambda)\right)^2 \tilde{G}^{>}_{\bar{D}}(k_0,\vec{k})\tilde{G}^{>}_{\sigma}(q_0-k_0,\vec{q}-\vec{k}) \\
& -\frac{1}{2}\left(imG_\pi\right)^2 \int \frac{d^4k}{(2\pi)^4}\left(F(\vec{k};\Lambda)\right)^2 \tilde{G}^{<}_{\bar{D}}(k_0,\vec{k})\tilde{G}^{<}_{\sigma}(q_0-k_0,\vec{q}-\vec{k}) \\
= \ & \frac{1}{2}\left(imG_\pi\right)^2 \int \frac{d^4k}{(2\pi)^4}\left(F(\vec{k};\Lambda)\right)^2 \theta(k_0)\rho_{\bar{D}}(k_0,\vec{q})\theta(q_0-k_0)\rho_{\sigma}(q_0-k_0,\vec{q}-\vec{k}) \\
& -\frac{1}{2}\left(imG_\pi\right)^2 \int \frac{d^4k}{(2\pi)^4}\left(F(\vec{k};\Lambda)\right)^2 \theta(-k_0)\rho_{\bar{D}}(k_0,\vec{k})\theta(-q_0+k_0)\rho_{\sigma}(q_0-k_0,\vec{q}-\vec{k}) \\
= \ & -\frac{1}{2}m^2G^2_\pi \int \frac{d^3k}{(2\pi)^3}\left(F(\vec{k};\Lambda)\right)^2 \\
& \times \frac{1}{2E^{\bar{D}}_k}\left\{\theta(q_0-E^{\bar{D}}_k)\rho_{\sigma}(q_0-E^{\bar{D}}_k,\vec{q}-\vec{k}) + \theta(-E^{\bar{D}}_k-q_0)\rho_{\sigma}(q_0+E^{\bar{D}}_k,\vec{q}-\vec{k})\right\} \ ,
\end{aligned} \tag{4.17}$$

where $E^{\bar{D}}_k$ is defined by $E^{\bar{D}}_k = \sqrt{|\vec{k}|^2 + m^2_{\bar{D}}}$. The real part of the retarded self-energy is derived by means of the subtracted dispersion relation in Eq. (4.8), and we can complete a calculation of the retarded self-energy in Fig. 4.3 (1a). Applications of this method to the remaining diagrams in Fig. 4.3 and Fig. 4.4 are straightforward, and we can complete the calculations of the retarded self-energy of $\bar{D}$ and $\bar{D}^*_0$ meson in nuclear matter.

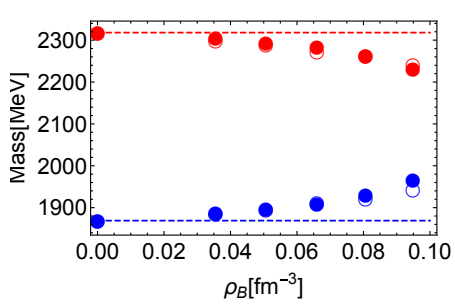

(a) Masses of $\bar{D}$ and $\bar{D}_0^*$ mesons.

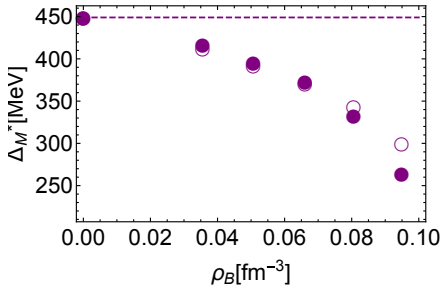

(b) Mass difference between $\bar{D}_0^*$ and $\bar{D}$ mesons.

Figure 4.5: (color online) The density dependence of (a) masses of $\bar{D}$ and $\bar{D}_0^*$ mesons and (b) that of mass difference between $\bar{D}_0^*$ and $\bar{D}$ mesons. The red filled circles and the blue filled circles in (a) denote the masses of $\bar{D}_0^*$ meson and $\bar{D}$, respectively, with Fock-type one-loop corrections as well as the mean field and Hartree-type one-loop corrections. The open circles in (a) represent the results with mean field alone. In a similar way, the filled purple circles in (b) denote the mass difference between $\bar{D}_0^*$ and $\bar{D}$ mesons with Fock-type one-loop corrections as well as the mean field and Hartree-type one-loop corrections, while the open ones denote that with mean field alone. The dashed horizontal lines correspond to the vacuum values put as references.

The resultant density dependence of masses of $\bar{D}$ and $\bar{D}_0^*$ mesons are plotted in Fig. 4.5 (a). Defining

$$\hat{m}_{\bar{D}} \equiv m - \frac{G_\pi}{2}(\sigma_0 + \delta\sigma_0) - \frac{\Delta_{\bar{D}}}{2} \ , \tag{4.18}$$

the mass of $\bar{D}$ meson is defined by the solution of $q_0^2 - \hat{m}_{\bar{D}}^2 - \mathrm{Re}\tilde{\Sigma}_{\bar{D}}(q_0, \vec{0}) = 0$ directly obtained by using a relation $\mathrm{Re}\tilde{\Sigma}_{\bar{D}}(q_0, \vec{0}) = \mathrm{Re}\tilde{\Sigma}^R_{\bar{D}}(q_0, \vec{0})$. The mass of $\bar{D}_0^*$ meson is defined by the value of energy at which maximum of its spectral function is realized [1]. The red filled circles and the blue filled circles in Fig. 4.5 (a) denote the masses of $\bar{D}_0^*$ meson and $\bar{D}$ meson, respectively, with Fock-type one-loop corrections as well as the mean field and Hartree-type one-loop corrections. The open circles in Fig. 4.5 (a) represent the results with mean field alone. From this figure together with Fig. 4.2, we can find Fock-type corrections push down the mass of $\bar{D}$ meson while they push up the mass of $\bar{D}_0^*$ meson. As a result, the resulting masses behave rather similar to the results with mean field. I plot the density dependence of the mass difference between

[1] The spectral function for $\bar{D}_0^*$ meson will be calculated in Sec. 4.2.

$\bar{D}_0^*$ and $\bar{D}$ mesons in Fig. 4.5 (b). The filled purple circles in Fig. 4.5 (b) denote the mass difference between $\bar{D}_0^*$ and $\bar{D}$ mesons with Fock-type one-loop corrections as well as the mean field and Hartree-type one loop corrections, while the open ones denote that with mean field alone.

4.2 Spectral functions for $\bar{D}$ and $\bar{D}_0^*$ mesons in nuclear matter

In this section, I show spectral functions for $\bar{D}$ and $\bar{D}_0^*$ meson. The spectral functions are defined by the same manner as in Eq. (4.5):

$$\rho_{\bar{D}(\bar{D}_0^*)}(k_0, \vec{k}) = \frac{-2\mathrm{Im}\tilde{\Sigma}^R_{\bar{D}(\bar{D}_0^*)}(k_0, \vec{k})}{\left[k^2 - \hat{m}^2_{\bar{D}(\bar{D}_0^*)} - \mathrm{Re}\tilde{\Sigma}^R_{\bar{D}(\bar{D}_0^*)}(k_0, \vec{k})\right]^2 + \left[\mathrm{Im}\tilde{\Sigma}^R_{\bar{D}(\bar{D}_0^*)}(k_0, \vec{k})\right]^2} \ . \quad (4.19)$$

$\hat{m}_{\bar{D}_0^*}$ is defined by

$$\hat{m}_{\bar{D}_0^*} = m + \frac{G_\pi}{2}(\sigma_0 + \delta\sigma_0) - \frac{\Delta_{\bar{D}_0^*}}{2} \quad (4.20)$$

as in Eq. (4.18). I particularly pay attention to the spectral function for $\bar{D}_0^*$ meson since $\bar{D}_0^*$ mainly decays into its chiral partner $\bar{D}$ meson by emitting a pion in the vacuum, so that it is expected the spectral function for $\bar{D}_0^*$ meson shows characteristic changes when we access to nuclear matter.

The resultant spectral functions for $\bar{D}_0^*$ meson at rest $\vec{q} = \vec{0}$ at several densities are shown in Fig. 4.6. The dashed curve is the spectral function in the vacuum, and colored curves are the obtained results. The vertical dotted lines refer to the threshold of $\bar{D} + \pi$ at each density. In this figure, we can find three peaks. The first peak corresponds to the resonance state of $\bar{D}_0^*$ meson. This peak shifts to the lower energy as the density increases which explicitly shows the reduction of mass of $\bar{D}_0^*$ meson as indicated by red circles in Fig. 4.5 (a). Also, this peak gets broadened and its hight gets suppressed. This is essentially caused by collisions with nucleons surrounding the $\bar{D}_0^*$ meson (collisional broadening) so that this effect is enhanced as the density increases. The second peak is identified as a threshold enhancement, and its peak position shifts to the higher energy regime as we increase the density. This peak suggests there is a virtual state, i.e., I expect we can find a pole on the real q_0 axis below the threshold in the second Riemann sheet. This state is made by an attractive force between $\bar{D}$ meson and pion. As the density increases, the level

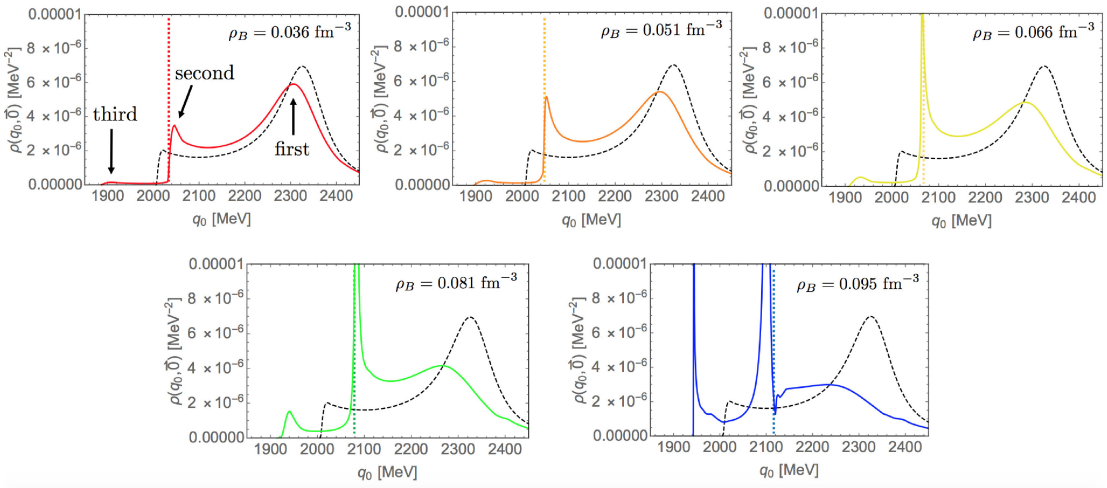

Figure 4.6: (color online) The spectral functions for $\bar{D}_0^*$ meson with vanishing momentum $\vec{q} = \vec{0}$ at $\rho_B = 0.036\,\mathrm{fm}^{-3}, 0.051\,\mathrm{fm}^{-3}, 0.066\,\mathrm{fm}^{-3}, 0.081\,\mathrm{fm}^{-3}, 0.095\,\mathrm{fm}^{-3}$. The dashed curve is the spectral function in the vacuum, and colored curves are the obtained results. The vertical dotted lines refer to the threshold of $\bar{D} + \pi$ at each density. The detail is given in the text.

difference between the bare mass of $\bar{D}_0^*$ meson ($m_{\bar{D}_0^*}$) and threshold of $\bar{D} + \pi$ gets small by the partial restoration of chiral symmetry, which causes an enlargement of level repulsion between these two levels. As a result, the attractive force between $\bar{D}$ meson and pion is strengthened, and the threshold enhancement is enhanced as the density increases. I should note that I expect a bound state of $\bar{D}\pi$ state appears at $\rho_B = 0.095$ fm^{-3} since the peak stands below the threshold. The third peak is regarded as the Landau damping. This bump is caused by scattering between $\bar{D}_0^*$ meson and a nucleon in medium as diagrammatically shown in Fig. 4.7, and gets enhanced as we increase the density.

The figures in Fig. 4.6 suggest that the threshold enhancement provide us with useful information of the partial restoration of chiral symmetry in real experiments since this peak is so sharp and remarkably enhanced. Furthermore, this peak stands at or near the threshold of $\bar{D}+\pi$, which tells us directly the sum of mass of $\bar{D}$ meson and pion.

I show the spectral function for $\bar{D}$ meson at $\rho_B = 0.066$ fm^{-3} with $\vec{q} = \vec{0}$ in Fig. 4.8. The dashed curve is the spectral function in the vacuum, and the yellow colored curve is the result. Some bumps correspond to the opening of some channels. Note that the magnitude of spectral function for $\bar{D}$ meson is smaller than that for $\bar{D}_0^*$

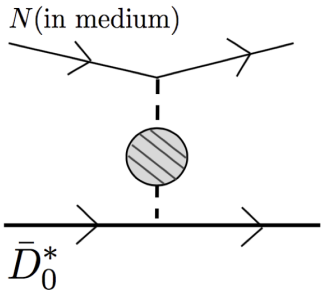

Figure 4.7: A diagrammatical representation of the Landau damping.

meson. This difference reflects that $\bar{D}_0^*$ meson can decay within the strong interaction while $\bar{D}$ meson can only decay by the weak interaction.

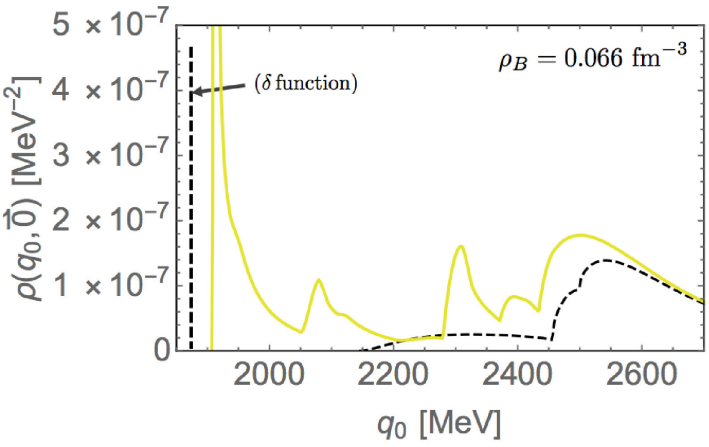

Figure 4.8: (color online) A spectral function for $\bar{D}$ meson at $\rho_B = 0.066$ fm^{-3} with $\vec{q} = \vec{0}$. The dashed curve is the spectral function in the vacuum, and yellow colored curve is the result.

Chapter 5

Modifications of $\bar{D}$ mesons in nuclear matter by the parity doublet model

The linear sigma model I have employed throughout Chap. 4 provides us with fruitful information on tendency of chiral restoration and changes of $\bar{D}$ mesons at low density. The use of this model is, however, limited to lower density than the normal nuclear matter density. In this chapter, I utilize the parity doublet model [37] which can reproduce properties of nuclear matter in a consistent way and study the spectral function for $\bar{D}_0^*$ meson at the nuclear matter density. In Sec. 5.1, I give the detailed explanation of an idea of parity doublet model. In Sec. 5.2, I construct nuclear matter with a mean field approximation in this model and determine parameters. In Sec. 5.3, I study a spectral function for $\bar{D}_0^*$ meson by the parity doublet model.

5.1 Parity doublet model

Quarks are such elementary particles that they belong to the fundamental representation of $SU(2)_L \times SU(2)_R$ chiral representation:

$$q = q_L + q_R \sim (\mathbf{2}, \mathbf{1}) \oplus (\mathbf{1}, \mathbf{2}) \ . \tag{5.1}$$

In this equation, q is a quark field, q_L (q_R) is a corresponding left-handed (right-handed) quark, and the number in left (right) component in the bracket refers to the representation of $SU(2)_L$ ($SU(2)_R$) chiral group. Namely, q_L and q_R transforms under the $SU(2)_L \times SU(2)_R$ chiral transformation as

$$q_L \to g_L q_L \ , \quad q_R \to g_R q_R \ . \tag{5.2}$$

In a first approximation, a nucleon is composed of three light quarks, so that its chiral representation can take three patterns as

$$\begin{aligned} N \sim q \otimes q \otimes q &\sim \big((\mathbf{2},\mathbf{1}) \oplus (\mathbf{1},\mathbf{2})\big)^3 \\ &= 5\left[(\mathbf{2},\mathbf{1}) \oplus (\mathbf{1},\mathbf{2})\right] + 3\left[(\mathbf{3},\mathbf{2}) \oplus (\mathbf{2},\mathbf{3})\right] \oplus \left[(\mathbf{4},\mathbf{1}) \oplus (\mathbf{1},\mathbf{4})\right] \ . \end{aligned} \tag{5.3}$$

Here, we take the $(\mathbf{2},\mathbf{1}) \oplus (\mathbf{1},\mathbf{2})$ representation for the nucleon. We further take that a Δ baryon belongs to $(\mathbf{3},\mathbf{2}) \oplus (\mathbf{2},\mathbf{3})$ representation since Δ baryon couples to the nucleon and pion strongly, and $N \sim (\mathbf{2},\mathbf{1}) \oplus (\mathbf{1},\mathbf{2})$ and $\pi \sim (\mathbf{2},\mathbf{2})$ which does not contain $(\mathbf{4},\mathbf{1}) \oplus (\mathbf{1},\mathbf{4})$.

As I have stated above, the nucleon belongs to $(\mathbf{2},\mathbf{1}) \oplus (\mathbf{1},\mathbf{2})$. One of the simple choice is $N_L \sim (\mathbf{2},\mathbf{1})$ and $N_R \sim (\mathbf{1},\mathbf{2})$, where N_L and N_R are defined in terms of an eigenvalue of a chirality γ_5 by $N_L = \frac{1-\gamma_5}{2}$ and $N_R = \frac{1+\gamma_5}{2}$, respectively. It is possible, however, that we take another choice: $N_L \sim (\mathbf{1},\mathbf{2})$ and $N_R \sim (\mathbf{2},\mathbf{1})$. Namely, we can introduce two types of the nucleon fields N_1 and N_2 which transform under the $SU(2)_L \times SU(2)_R$ chiral transformation as

$$\begin{aligned} N_{1L} \to g_L N_{1L} \quad &, \quad N_{1R} \to g_R N_{1R} \\ N_{2L} \to g_R N_{2L} \quad &, \quad N_{2R} \to g_L N_{2R} \ . \end{aligned} \tag{5.4}$$

The assignment for the nucleon N_2 is called a "mirror assignment" [43, 44, 45, 46]. An effective model based on the mirror assignment is referred to as the parity doublet model. I should remind that the subscripts L and R are defined by the eigenvalues of the chirality

$$N_{1(2),L} = \frac{1-\gamma_5}{2} N_{1(2)} \ , \quad N_{1(2),R} = \frac{1+\gamma_5}{2} N_{1(2)} \ . \tag{5.5}$$

The chirality is related to the parity, so that it is expected that we obtain a characteristic structure in terms of the parity-eigenstate when we take the mirror assignment. In order to see it, let us construct an effective Lagrangian which is invariant under the $SU(2)_L \times SU(2)_R$ chiral transformation, parity and charge conjugation. Regarding the parity transformation, I assign the following transformation properties:

$$\begin{aligned} N_{1L}(x) \to N_{1R}(x_p) \quad &, \quad N_{1L}(x) \to N_{1R}(x_p) \\ N_{2R}(x) \to -N_{2L}(x_p) \quad &, \quad N_{2L}(x) \to -N_{2R}(x_p) \ . \end{aligned} \tag{5.6}$$

For N_2, I put an unfamiliar phase -1 under the parity transformation. This phase is, however, does not contain physical meanings since N_1 and N_2 themselves are not

regarded as physical states as we will see soon. This phase is just put for later use. The nucleon part of the effective Lagrangian up to the first order of derivative can be obtained as [38]

$$\begin{aligned}\mathcal{L}_N &= \bar{N}_{1R}i\partial\!\!\!/ N_{1R} + \bar{N}_{1L}i\partial\!\!\!/ N_{1L} + \bar{N}_{2R}i\partial\!\!\!/ N_{2R} + \bar{N}_{2L}i\partial\!\!\!/ N_{2L} \\ &\quad -m_0\left[\bar{N}_{1L}N_{2R} - \bar{N}_{1R}N_{2L} - \bar{N}_{2L}N_{1R} + \bar{N}_{2R}N_{1L}\right] \\ &\quad -g_1\left[\bar{N}_{1R}M^\dagger N_{1L} + \bar{N}_{1L}MN_{1R}\right] - g_2\left[\bar{N}_{2R}MN_{2L} + \bar{N}_{2L}M^\dagger N_{2R}\right] \\ &\quad -ih_1\left[\bar{N}_{1L}(M\partial\!\!\!/ M^\dagger - \partial\!\!\!/ MM^\dagger)N_{1L} + \bar{N}_{1R}(M^\dagger\partial\!\!\!/ M - \partial\!\!\!/ M^\dagger M)N_{1R}\right] \\ &\quad -ih_2\left[\bar{N}_{2R}(M\partial\!\!\!/ M^\dagger - \partial\!\!\!/ MM^\dagger)N_{2R} + \bar{N}_{2L}(M^\dagger\partial\!\!\!/ M - \partial\!\!\!/ M^\dagger M)N_{2L}\right] \ ,\end{aligned} \tag{5.7}$$

where M is the chiral field defined by Eq. (2.19) and m_0, g_1, g_2, h_1 and h_2 are real parameters. Under the spontaneous breakdown of chiral symmetry, σ meson field is replaced by its VEV σ_0 and a resultant Lagrangian is

$$\begin{aligned}\mathcal{L}_N &= \bar{N}_{1R}i\partial\!\!\!/ N_{1R} + \bar{N}_{1L}i\partial\!\!\!/ N_{1L} + \bar{N}_{2R}i\partial\!\!\!/ N_{2R} + \bar{N}_{2L}i\partial\!\!\!/ N_{2L} \\ &\quad -m_0\left[\bar{N}_{1L}N_{2R} - \bar{N}_{1R}N_{2L} - \bar{N}_{2L}N_{1R} + \bar{N}_{2R}N_{1L}\right] \\ &\quad -g_1\sigma_0\left[\bar{N}_{1R}N_{1L} + \bar{N}_{1L}N_{1R}\right] - g_2\sigma_0\left[\bar{N}_{2R}N_{2L} + \bar{N}_{2L}N_{2R}\right] \\ &= \bar{N}_1 i\partial\!\!\!/ N_1 + \bar{N}_2 i\partial\!\!\!/ N_2 - m_0\left[\bar{N}_1\gamma_5 N_2 - \bar{N}_2\gamma_5 N_1\right] \\ &\quad -g_1\sigma_0\bar{N}_1N_1 - g_2\sigma_0\bar{N}_2N_2 \ ,\end{aligned} \tag{5.8}$$

where we have neglected fluctuations of σ meson and pion. The Lagrangian (5.8) shows that a mass matrix is not diagonalized in terms of N_1 and N_2. By introducing two mass eigenstates N_+ and N_- via

$$\begin{pmatrix} N_+ \\ N_- \end{pmatrix} = \begin{pmatrix} \cos\theta & \gamma_5\sin\theta \\ -\gamma_5\sin\theta & \cos\theta \end{pmatrix}\begin{pmatrix} N_1 \\ N_2 \end{pmatrix} \ , \tag{5.9}$$

this mass matrix can be diagonalized by taking the mixing angle θ to satisfy

$$\tan 2\theta = \frac{2m_0}{(g_1+g_2)\sigma_0} \ . \tag{5.10}$$

In this case, the Lagrangian in Eq. (5.8) is rewritten into

$$\mathcal{L}_N = \bar{N}_+ i\partial\!\!\!/ N_+ + \bar{N}_- i\partial\!\!\!/ N_- - m_+\bar{N}_+N_+ - m_-\bar{N}_-N_- \ , \tag{5.11}$$

where the masses of N_+ and N_- are derived as

$$m_+ \equiv \frac{1}{2}\left[\sqrt{(g_1+g_2)^2\sigma_0^2 + 4m_0^2} - (g_2-g_1)\sigma_0\right] \tag{5.12}$$

$$m_- \equiv \frac{1}{2}\left[\sqrt{(g_1+g_2)^2\sigma_0^2 + 4m_0^2} + (g_2-g_1)\sigma_0\right] \ . \tag{5.13}$$

Note that the definition of N_+ and N_- in Eq. (5.9) together with the parity transformations of N_1 and N_2 in Eq. (5.6) leads to the parity transformation laws of N_+ and N_- as

$$N_+(x) \xrightarrow{P} \gamma_0 N_+(x_p) \ , \quad N_-(x) \xrightarrow{P} -\gamma_0 N_-(x_p) \ . \tag{5.14}$$

Namely, the parity eigenvalue of N_+ is $+1$ while that of N_- is -1. This fact allows us to assign N_+ and N_- as the nucleon $N(939)$ and $N^*(1535)$, respectively. Another feature of mirror assignment is that we can get a relation between the mass splitting of N_- and N_+ and the VEV of σ meson as

$$m_- - m_+ = (g_2 - g_1)\sigma_0 \ . \tag{5.15}$$

This relation is often referred to as the extended Goldberger-Treiman relation since this is a naive extension of the original Goldberger-Treiman relation.

When we utilized a polar decomposition with respect to the pion as

$$M = \sigma U = \sigma \exp\left(i\frac{\pi^a \tau^a}{f_\pi}\right) \ , \tag{5.16}$$

and expand the Lagrangian (5.7) up to the second order of meson fields, we can find

$$\begin{aligned}
\mathcal{L}_N \ = \ & \bar{N}_+(i\partial\!\!\!/ + \mu_B\gamma^0 - g_\omega \omega\!\!\!/)N_+ + \bar{N}_-(i\partial\!\!\!/ + \mu_B\gamma^0 - g_\omega \omega\!\!\!/)N_- - m_+\bar{N}_+N_+ - m_-\bar{N}_-N_- \\
& - g_{NN\sigma}\bar{N}_+\sigma N_+ - g_{NN\pi}\bar{N}_+ i\gamma_5\pi_r N_+ + g_{NN^*\sigma}\bar{N}_+\gamma_5\sigma N_- + g_{NN^*\pi}\bar{N}_+ i\pi_r N_- \\
& - g_{NN^*\sigma}\bar{N}_-\gamma_5\sigma N_+ - g_{NN^*\pi}\bar{N}_- i\pi_r N_+ - g_{N^*N^*\sigma}\bar{N}_-\sigma N_- - g_{N^*N^*\pi}\bar{N}_- i\gamma_5\pi_r N_- \\
& + \frac{g_{NN\sigma}}{2\sigma_0}\bar{N}_+\pi_r^2 N_+ - \frac{g_{NN^*\sigma}}{2\sigma_0}\bar{N}_+\gamma_5\pi_r^2 N_- + \frac{g_{NN^*\sigma}}{2\sigma_0}\bar{N}_-\gamma_5\pi_r^2 N_+ + \frac{g_{N^*N^*\sigma}}{2\sigma_0}\bar{N}_-\pi_r^2 N_- \\
& + 2\sigma_0 h_{NN\pi}\bar{N}_+\partial\!\!\!/\pi_r\gamma_5 N_+ + 2\sigma_0 h_{NN^*\pi}\bar{N}_+\partial\!\!\!/\pi_r N_- + 2\sigma_0 h_{NN^*\pi}\bar{N}_-\partial\!\!\!/\pi_r N_+ + 2\sigma_0\bar{N}_-\partial\!\!\!/\pi_r\gamma_5 N_- \\
& - i f_\pi h_{NN\pi\pi}\bar{N}_+[\pi_r, \partial\!\!\!/\pi_r]N_+ - i f_\pi h_{NN^*\pi\pi}\bar{N}_+[\pi_r, \partial\!\!\!/\pi_r]\gamma_5 N_- \\
& - i f_\pi h_{NN^*\pi\pi}\bar{N}_+[\pi_r, \partial\!\!\!/\pi_r]\gamma_5 N_- - i f_\pi h_{N^*N^*\pi\pi}\bar{N}_-[\pi_r, \partial\!\!\!/\pi_r]N_- \\
& + \cdots
\end{aligned} \tag{5.17}$$

in terms of N_+ and N_- fields under the spontaneous breakdown of chiral symmetry. In Eq. (5.17), we have defined

$$\pi = Z^{1/2}\pi_r \quad \text{with } Z = \frac{f_\pi^2}{\sigma_0^2} \tag{5.18}$$

so as to renormalize the kinetic term of pion properly, and the coupling constants are

$$
\begin{aligned}
g_{NN\sigma} &= \frac{1}{2}(g_1-g_2)+\frac{1}{2}(g_1+g_2)\frac{(g_1+g_2)\sigma_0}{\sqrt{(g_1+g_2)^2\sigma_0^2+4m_0^2}} \\
g_{NN\pi} &= \frac{1}{2}(g_1+g_2)+\frac{1}{2}(g_1-g_2)\frac{(g_1+g_2)\sigma_0}{\sqrt{(g_1+g_2)^2\sigma_0^2+4m_0^2}} \\
g_{NN^*\sigma} &= (g_1+g_2)\frac{m_0}{\sqrt{(g_1+g_2)^2\sigma_0^2+4m_0^2}} \\
g_{NN^*\pi} &= (g_1-g_2)\frac{m_0}{\sqrt{(g_1+g_2)^2\sigma_0^2+4m_0^2}} \\
g_{N^*N^*\sigma} &= -\frac{1}{2}(g_1-g_2)+\frac{1}{2}(g_1+g_2)\frac{(g_1+g_2)\sigma_0}{\sqrt{(g_1+g_2)^2\sigma_0^2+4m_0^2}} \\
g_{N^*N^*\pi} &= -\frac{1}{2}(g_1+g_2)+\frac{1}{2}(g_1-g_2)\frac{(g_1+g_2)\sigma_0}{\sqrt{(g_1+g_2)^2\sigma_0^2+4m_0^2}} \\
h_{NN\pi} &= \frac{1}{2}(h_1-h_2)+\frac{1}{2}(h_1+h_2)\frac{(g_1+g_2)\sigma_0}{\sqrt{(g_1+g_2)^2\sigma_0^2+4m_0^2}} \\
h_{NN^*\pi} &= -(h_1+h_2)\frac{m_0}{\sqrt{(g_1+g_2)^2\sigma_0^2+4m_0^2}} \\
h_{N^*N^*\pi} &= \frac{1}{2}(h_1-h_2)-\frac{1}{2}(h_1+h_2)\frac{(g_1+g_2)\sigma_0}{\sqrt{(g_1+g_2)^2\sigma_0^2+4m_0^2}} \\
h_{NN\pi\pi} &= \frac{1}{2}(h_1+h_2)+\frac{1}{2}(h_1-h_2)\frac{(g_1+g_2)\sigma_0}{\sqrt{(g_1+g_2)^2\sigma_0^2+4m_0^2}} \\
h_{NN^*\pi\pi} &= -(h_1-h_2)\frac{m_0}{\sqrt{(g_1+g_2)^2\sigma_0^2+4m_0^2}} \\
h_{N^*N^*\pi\pi} &= \frac{1}{2}(h_1+h_2)-\frac{1}{2}(h_1-h_2)\frac{(g_1+g_2)\sigma_0}{\sqrt{(g_1+g_2)^2\sigma_0^2+4m_0^2}} \ . \qquad (5.19)
\end{aligned}
$$

Note that we have added baryon number chemical potentials μ_B to the nucleon and $N^*(1535)$ since we will access to density system. ω meson is also put as a chiral singlet particle in $SU(2)_L \times SU(2)_R$ to determine a density dependence of our model self-consistently.

The mesonic Lagrangian is introduced for the present analysis by including a

six-point interaction of meson fields as [37]

$$\begin{aligned}\mathcal{L}_M &= \frac{1}{4}\mathrm{tr}[\partial_\mu M \partial^\mu M^\dagger] + \frac{\bar{\mu}^2}{4}\mathrm{tr}[MM^\dagger] - \frac{\lambda}{16}(\mathrm{tr}[MM^\dagger])^2 + \frac{\lambda_6}{48}(\mathrm{tr}[MM^\dagger])^3 + \frac{1}{4}\bar{m}\epsilon\mathrm{tr}[M+M^\dagger] \\ &\quad -\frac{1}{4}\omega_{\mu\nu}\omega^{\mu\nu} + \frac{1}{2}m_\omega^2\omega_\mu\omega^\mu \ ,\end{aligned} \tag{5.20}$$

where $\omega_{\mu\nu} = \partial_\mu\omega_\nu - \partial_\nu\omega_\mu$ is added to create a kinetic term of ω meson and m_ω is the ω meson mass. This Lagrangian except for the last term is invariant under the $SU(2)_L \times SU(2)_R$ chiral transformation, and this last term is added to reproduce the finite pion mass. With the same way in obtaining Eq. (5.17), the mesonic part of the Lagrangian (5.20) is expanded as

$$\begin{aligned}\mathcal{L}_M &= \frac{1}{2}\partial_\mu\sigma\partial^\mu\sigma + \frac{1}{2}\partial_\mu\pi_r^a\partial^\mu\pi_r^a + \frac{1}{2}\bar{\mu}^2(\sigma_0+\sigma)^2 \\ &\quad -\frac{1}{4}\lambda(\sigma_0+\sigma)^4 + \frac{1}{6}\lambda_6(\sigma_0+\sigma)^6 + \bar{m}\epsilon\sigma_0 - \frac{1}{2}\frac{\bar{m}\epsilon}{\sigma_0}\pi_r^a\pi_r^a + \cdots \ .\end{aligned} \tag{5.21}$$

The Lagrangians in Eqs. (5.17) and (5.21) define our model.

5.2 Construction of nuclear matter and parameter determination

In this section, I determine the parameters in Eqs. (5.17) and (5.21). Some input parameters are summarized in Table. 5.1. In the present analysis, I utilize the nucleon mass, $N^*(1535)$ mass, pion mass, ω meson mass, pion decay constant, $\Gamma_{N^*\to N\pi}$, and the nucleon axial-charge (g_A) as inputs in the vacuum. In addition, I use saturation density, binding energy, incompressibility as inputs in nuclear matter. I list them in Table. 5.2. I should note that we have an additional condition of $\frac{\partial}{\partial\rho_B}(E/A - m_+^{\mathrm{vac}})|_{\rho_B^*} = 0$ to reproduce the saturation behavior (A is the mass number). Therefore, we need to obtain thermodynamical quantities within our model and describe nuclear matter.

From the Lagrangians in Eqs. (5.17) and (5.21), we can find a thermodynamic potential Ω with mean fields of σ meson (σ_0) and time-component of ω meson (ω_0)

$m_+^{\rm vac}$(MeV)	$m_-^{\rm vac}$(MeV)	m_π(MeV)	m_ω(MeV)	f_π(MeV)	$\Gamma_{N^*\to N\pi}$(MeV)	g_A
939	1535	140	783	93	75	1.27

Table 5.1: Input parameters by properties in the vacuum. In this table, $m_+^{\rm vac}$, $m_-^{\rm vac}$, m_π, m_ω, f_π, $\Gamma_{N^*\to N\pi}$, g_A represent the nucleon mass, $N^*(1535)$ mass, pion mass, ω meson mass, decay width of $N^* \to N\pi$, nucleon axial charge, respectively.

$\rho_B^*({\rm fm}^{-3})$	$E/A - m_+^{\rm vac}$(MeV)	K(MeV)
0.16	-16	240

Table 5.2: Input parameters by properties in nuclear matter. In this table, ρ_B^*, E, A, K represent the normal nuclear matter density, total energy of the system, mass number, incompressibility, respectively. I should note that we have additional condition of $\frac{\partial}{\partial\rho_B}(E/A - m_+^{\rm vac})|_{\rho_B^*} = 0$ to reproduce the saturation nature.

as

$$\begin{aligned}
\Omega &= -\frac{1}{\beta}\ln Z \\
&= -i\frac{1}{\beta}{\rm Tr}\ln(i\partial\!\!\!/ + \mu_B^*\gamma_0 - m_+) - i\frac{1}{\beta}{\rm Tr}\ln(i\partial\!\!\!/ + \mu_B^*\gamma_0 - m_-) \\
&\quad + \frac{1}{\beta}\int_0^\beta d\tau \int d^3x \frac{1}{2}m_\omega^2\omega_0^2 + \frac{1}{2}\bar{\mu}^2\sigma_0^2 - \frac{1}{4}\lambda\sigma_0^4 + \frac{1}{6}\lambda_6\sigma_0^6 + \bar{m}\epsilon\sigma_0 \\
&\stackrel{\beta\to\infty}{\to} \sum_{i=+,-}\frac{V}{4\pi^2}\left\{\frac{2}{3}\sqrt{k_{Fi}^2+m_i^2}k_{Fi}^3 - \sqrt{k_{Fi}^2+m_i^2}k_{Fi}m_i^2 + m_i^4\ln\left(\frac{k_{Fi}+\sqrt{k_{Fi}^2+m_i^2}}{m_i}\right)\right\} \\
&\quad + V\left(\frac{1}{2}m_\omega^2\omega_0^2 + \frac{1}{2}\bar{\mu}^2\sigma_0^2 - \frac{1}{4}\lambda\sigma_0^4 + \frac{1}{6}\lambda_6\sigma_0^6 + \bar{m}\epsilon\sigma_0\right) ,
\end{aligned} \tag{5.22}$$

where $\beta = 1/T$ is the inverse of temperature and V is the volume of the system. Both of them should be taken to be infinity since we study on infinite volume nuclear matter at zero temperature. Correspondingly, V is not regarded as a variable in our approach. I note that I assume such parity non-vanishing condensates that mean fields of pion and space-components of ω meson do not have their non-zero values. μ_B^* is the effective chemical potential defined by $\mu_B^* = \mu_B - g_\omega\omega_0$ and k_{F+} and k_{F-} are the Fermi momenta of N_+ and N_- defined by $k_{F+} = \sqrt{\mu_B^{*2} - m_+^2}$ and $k_{F-} = \sqrt{\mu_B^{*2} - m_-^2}$, respectively. The mean fields σ_0 and ω_0 satisfy the stationary

conditions $\frac{\partial\Omega}{\partial\sigma_0}=0, \frac{\partial\Omega}{\partial\omega_0}=0$ which are of the forms

$$\begin{aligned} & -\bar{\mu}^2\sigma_0+\lambda\sigma_0^3-\lambda_6\sigma_0^5-\bar{m}\epsilon \\ = \; & 4\left((g_2-g_1)-\frac{(g_1+g_2)^2\sigma_0}{\sqrt{(g_1+g_2)^2\sigma_0^2+4m_0^2}}\right)\int^{k_{F+}}\frac{d^3k}{(2\pi)^3}\frac{m_+}{2\sqrt{k^2+m_+^2}} \\ & -4\left((g_2-g_1)+\frac{(g_1+g_2)^2\sigma_0}{\sqrt{(g_1+g_2)^2\sigma_0^2+4m_0^2}}\right)\int^{k_{F-}}\frac{d^3k}{(2\pi)^3}\frac{m_-}{2\sqrt{k^2+m_-^2}} \; , \end{aligned} \tag{5.23}$$

and

$$\begin{aligned} \omega_0 &= \frac{g_\omega}{m_\omega^2}\rho_B \\ &= \frac{g_\omega}{m_\omega^2}\left(\frac{2}{3\pi^2}k_{F+}^3+\frac{2}{3\pi^2}k_{F-}^3\right) \; . \end{aligned} \tag{5.24}$$

The pressure P is given by

$$\begin{aligned} P &= -\Omega/V-P_{\rm vacuum} \\ &= \sum_{i=+,-}\frac{1}{4\pi^2}\left\{\frac{2}{3}\sqrt{k_{Fi}^2+m_i^2}k_{Fi}^3-\sqrt{k_{Fi}^2+m_i^2}k_{Fi}m_i^2+m_i^4\ln\left(\frac{k_{Fi}+\sqrt{k_{Fi}^2+m_i^2}}{m_i}\right)\right\} \\ & +\frac{1}{2}m_\omega^2\omega_0^2+\frac{1}{2}\bar{\mu}^2\sigma_0^2-\frac{1}{4}\lambda\sigma_0^4+\frac{1}{6}\lambda_6\sigma_0^6+\bar{m}\epsilon\sigma_0-\left\{\frac{1}{2}\bar{\mu}^2f_\pi^2-\frac{1}{4}\lambda f_\pi^4+\frac{1}{6}\lambda_6 f_\pi^6+\bar{m}\epsilon f_\pi\right\} \; , \end{aligned} \tag{5.25}$$

and the averaged energy per-volume ϵ is

$$\begin{aligned} \epsilon &= -\frac{1}{V}\frac{\partial}{\partial\beta}\ln Z+\mu_B\frac{A}{V}-\epsilon_{\rm vacuum} \\ &= 4\int\frac{d^3k}{(2\pi)^3}(E_k^+-\mu_B^*)\theta(k_F^+-|\vec{k}|)+4\mu_B\int\frac{d^3k}{(2\pi)^3}\theta(k_F^+-|\vec{k}|) \\ & -\frac{1}{2}m_\omega^2\omega_0^2-\frac{1}{2}\bar{\mu}^2\sigma_0^2+\frac{1}{4}\lambda\sigma_0^4-\frac{1}{6}\lambda_6\sigma_0^6-\bar{m}\epsilon\sigma_0+\left\{\frac{1}{2}\bar{\mu}^2f_\pi^2-\frac{1}{4}\lambda f_\pi^4+\frac{1}{6}\lambda_6 f_\pi^6+\bar{m}\epsilon f_\pi\right\} \\ &= \sum_{i=+,-}\frac{1}{4\pi^2}\left\{k_{Fi}\sqrt{k_{Fi}^2+m_i^2}(2k_{Fi}^2+m_i^2)-m_i^4\ln\left(\frac{k_{Fi}+\sqrt{k_{Fi}^2+m_i^2}}{m_i}\right)\right\} \\ & +\frac{1}{2}m_\omega^2\omega_0^2-\frac{1}{2}\bar{\mu}^2\sigma_0^2+\frac{1}{4}\lambda\sigma_0^4-\frac{1}{6}\lambda_6\sigma_0^6-\bar{m}\epsilon\sigma_0+\left\{\frac{1}{2}\bar{\mu}^2f_\pi^2-\frac{1}{4}\lambda f_\pi^4+\frac{1}{6}\lambda_6 f_\pi^6+\bar{m}\epsilon f_\pi\right\} \; . \end{aligned} \tag{5.26}$$

In Eqs. (5.25) and (5.26), I have subtracted vacuum pressure

$$\begin{aligned} P_{\rm vacuum} &= -\frac{\Omega_{\rm vacuum}}{V} \\ &= \frac{1}{2}\bar{\mu}^2 f_\pi^2 - \frac{1}{4}\lambda f_\pi^4 + \frac{1}{6}\lambda_6 f_\pi^6 + \bar{m}\epsilon f_\pi \end{aligned} \tag{5.27}$$

and vacuum energy per-volume

$$\begin{aligned} \epsilon_{\rm vacuum} &= -\frac{1}{V}\frac{\partial}{\partial\beta}\ln Z\Big|_{\rm vacuum} \\ &= -\frac{1}{2}\bar{\mu}^2 f_\pi^2 + \frac{1}{4}\lambda f_\pi^4 - \frac{1}{6}\lambda_6 f_\pi^6 - \bar{m}\epsilon f_\pi \end{aligned} \tag{5.28}$$

to measure them from the appropriate ground state.

From Eq. (5.26), the binding energy of a nucleon in nuclear matter is easily calculated thanks to a relation of $E/A = \epsilon/\rho_B^*$. The saturation condition is reduced to

$$\begin{aligned} \frac{\partial}{\partial\rho_B}(E/A - m_+^{\rm vac})|_{\rho_B^*} &= V\left(\frac{\partial(\frac{E}{A})}{\partial A}\right)_V\Bigg|_{\rho_B^*} \\ &= V\,\frac{\left(\frac{\partial E}{\partial A}\right)_V A - E}{A^2}\Bigg|_{\rho_B^*} \\ &= V\,\frac{\mu_B A - E}{A^2}\Bigg|_{\rho_B^*} \\ &= \frac{V^2}{A^2}P|_{\rho_B^*} \\ &= 0\ , \end{aligned} \tag{5.29}$$

namely, only we need to do is to solve a simple equation

$$P|_{\rho_B^*} = 0\ . \tag{5.30}$$

In obtaining Eq. (5.29), we have made use of thermodynamic identities

$$dE = TdS - PdV + \mu_B dA \tag{5.31}$$

and

$$E = TS - PV + \mu_B A\ , \tag{5.32}$$

with $T = 0$ (T is the temperature and S is an entropy). The incompressibility is defined by

$$K = 9\rho_B^{*2}\frac{\partial^2}{\partial\rho_B^2}\left(\frac{E}{A}\right)_V\Big|_{\rho_B^*}\ , \tag{5.33}$$

and is rewritten into

$$\begin{aligned} K &= 9\left(\frac{\partial P}{\partial\rho_B}\right)_V\Big|_{\rho_B^*} \\ &= -9\left(\frac{\partial\Omega}{\partial A}\right)_V\Big|_{\rho_B^*} \\ &= -9\left(\frac{\partial\mu_B}{\partial A}\frac{\partial\Omega}{\partial\mu_B}\right)_V\Big|_{\rho_B^*} \\ &= 9\rho_B^*\left(\frac{\partial\mu_B}{\partial\rho_B}\right)_V\Big|_{\rho_B^*} \\ &= 9\rho_B^*\left\{\frac{1}{\mu_B^*(k_{F+}+k_{F-})}\left(\frac{\pi^2}{2}+\sum_{i=+,-}k_{Fi}m_i\frac{\partial m_i}{\partial\rho_B}\right)+\frac{g_\omega^2}{m_\omega^2}\right\}\Bigg|_{\rho_B^*}\ , \end{aligned} \tag{5.34}$$

where we have used other thermodynamical relations of

$$d\Omega = -SdT - PdV - Ad\mu_B \tag{5.35}$$

and

$$P = -\frac{1}{V}\Omega(T, V, \mu_B)\ . \tag{5.36}$$

With helps of above equations together with the stationary conditions in Eqs. (5.23) and (5.24), we can determine the parameters with several values of m_0 as in Table 5.3. I should note that only m_0 remains as a free parameter. In other words, the origin of mass of the nucleon cannot be determined since m_0 is the chiral invariant mass defined by a part of the nucleon mass which is invariant in terms of chiral symmetry as in Eq. (5.12).

In Fig. 5.1, I plot density dependences of the mean field σ_0 and mass of $N^*(1535)$ and the nucleon. In the present model, we can access to the normal nuclear matter density $\rho_B = 0.16\ \mathrm{fm}^{-3}$ respecting the nuclear matter properties listed in Table. 5.2 as indicated in this figure. The mean field σ_0 decreases as the density increases which reflects the partial restoration of chiral symmetry as was seen in the linear sigma

m_0 [MeV]	500	700	900
g_1	9.03	7.82	5.97
g_2	15.5	14.3	12.4
g_ω	6.75	6.22	3.49
$\hat{\bar{\mu}}^2$	73.5	30.8	1.74
λ	139	58.8	5.00
$\hat{\lambda}_6$	62.9	25.7	0.952
$\hat{h}_1$	0.108	0.127	0.145
$\hat{h}_2$	0.336	0.0473	$-$ 0.126

Table 5.3: Model parameters for a given value of m_0. The dimensionless parameters $\hat{\bar{\mu}}^2$, $\hat{\lambda}_6$ $\hat{h}_1$ and $\hat{h}_2$ are defined by $\hat{\bar{\mu}} = \bar{\mu}^2/f_\pi^2$, $\hat{\lambda}_6 = \lambda_6 \cdot f_\pi^2$, $\hat{h}_1 = h_1 \cdot f_\pi^2$ and $\hat{h}_2 = h_2 \cdot f_\pi^2$.

model. Accordingly, the mass of the nucleon drops and that of $N^*(1535)$ drops more rapidly, and the mass difference between them is also suppressed as we increase the density. This tendency is obviously understood by the extended Goldberger-Treiman relation of our model in Eq. (5.15).

5.3 Spectral function for $\bar{D}_0^*$ meson

In this section, I show spectral functions for $\bar{D}_0^*$ meson at normal nuclear matter density $\rho_B = 0.16$ fm^{-3} with some values of m_0. I include Hartree-type and Fock-type one-loop corrections in addition to the mean field for calculating the self-energy of $\bar{D}_0^*$, and the same procedure used in Chap. 4 is employed to get the spectral function.

For the propagator of pion, we need to include infinite sums of self-energies shown in Fig. 5.2 to preserve chiral symmetry in our calculation. In the analysis in this chapter, I take into account only $\bar{D}\pi$ loop in the calculation of the self-energy of $\bar{D}_0^*$ to avoid complexity. I confirm that this procedure gives a reasonable result for the spectral function for $\bar{D}_0^*$ meson numerically.

The resulting spectral functions with $m_0 = 500$ MeV, 700 MeV, 900 MeV are indicated in Fig. 5.3. The colored curves are the results, and dashed black curve is the spectral function in the vacuum. I take $\vec{q} = \vec{0}$ in this figure. We find two clear peaks in the spectral function which are regarded as a resonance of $\bar{D}_0^*$ state and a threshold enhancement. The physical meaning of them have been already provided in Chap. 4. In Fig. 5.3, we cannot get a clear bump of the Landau damping in contrast with the results in the linear sigma model in Chap. 4. As we can see, the

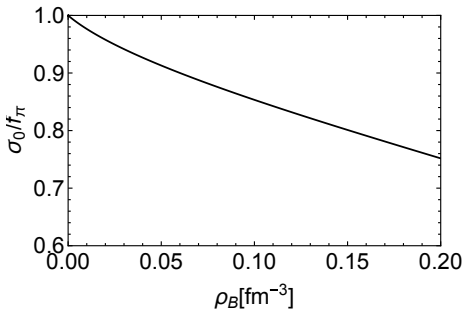

(a) Density dependence of σ_0.

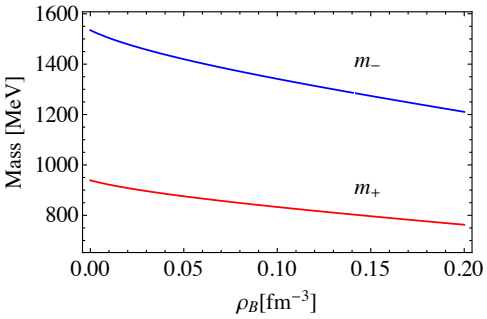

(b) Density dependence of m_+ and m_-.

Figure 5.1: (color online) Density dependence of (a) the mean field σ_0 and (b) mass of the nucleon and $N^*(1535)$.

resultant peak position of the $\bar{D}_0^*$ resonance (threshold enhancement) moves to the lower energy regime (higher energy regime) as we increase the value of m_0. This tendency is triggered since the larger the value of m_0 is taken, the faster the partial restoration of chiral symmetry is realized. I should note that the threshold of $\bar{D}+\pi$ is located at $q_0 = 2124$ MeV for $m_0 = 900$ MeV and the threshold enhancement stands below it, which suggests an existence of a bound state of $\bar{D}\pi$ state.

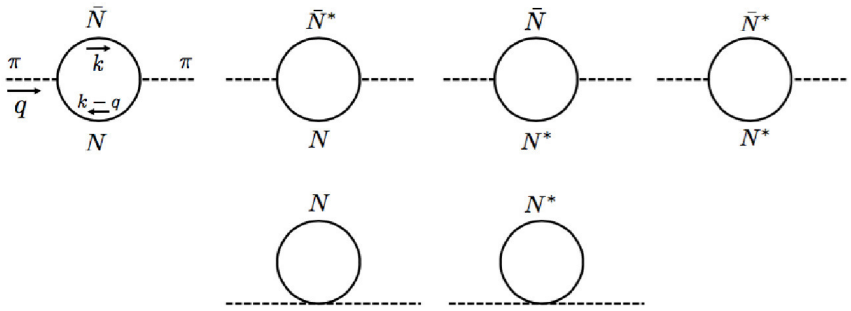

Figure 5.2: Self-energy for pion ($\tilde{\Sigma}_\pi(q_0, \vec{q})$)

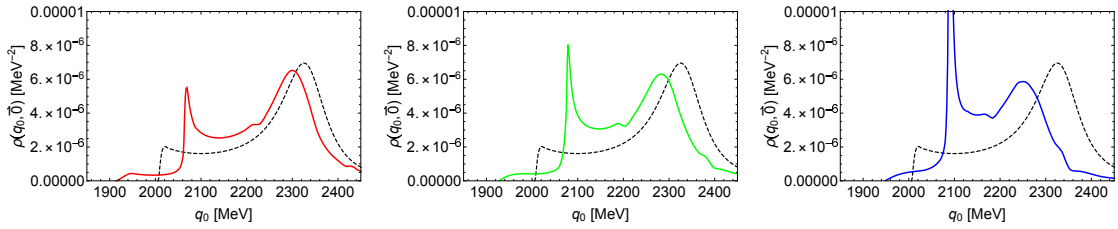

(a) $m_0 = 500$ MeV. (b) $m_0 = 700$ MeV. (c) $m_0 = 900$ MeV.

Figure 5.3: (color online) Spectral functions for $\bar{D}_0^*$ meson at $\rho_B = 0.16$ fm^{-3} and $\vec{q} = \vec{0}$ with (a) $m_0 = 500$ MeV, (b) $m_0 = 700$ MeV, (c) $m_0 = 900$ MeV. The colored curves are the results, and dashed black curve is the spectral function in the vacuum. The detail is given in the text.

Chapter 6

Conclusions

In this chapter, I give conclusions of this dissertation.

I investigate a possibility of $\bar{D}$ mesons as probes to explore the partial restoration of chiral symmetry in nuclear matter throughout this dissertation. An effective Lagrangian for $\bar{D}$ mesons is based on the Heavy Quark Spin Symmetry (HQSS) and the chiral partner structure. In order to investigate $\bar{D}$ mesons in nuclear matter respecting chiral symmetry correctly, we need to construct nuclear matter by a chiral model. I firstly employ the linear sigma model to describe nuclear matter since this model is one of the simplest chiral models, and we can fully study properties of $\bar{D}$ mesons at lower density regime qualitatively. I construct nuclear matter by a one-loop of a nucleon within the linear sigma model. In Fig. 3.3, I plot a density dependence of a mean field of σ meson (σ_0) which is regarded as an order parameter in terms of $SU(2)_L \times SU(2)_R$ chiral symmetry in the present analysis. This figure clearly shows that the value of σ_0 decreases as the baryon number density increases which represents a partial restoration of chiral symmetry in nuclear matter.

Modifications of $\bar{D}$ mesons in nuclear matter are induced by mediating σ meson and pion. I should emphasize that we must employ propagators for σ meson and pion which include infinite sums of the nucleon one-loops as depicted in Fig. 3.2 so as to respect chiral symmetry in our calculations in this regard. This is because our new ground state is defined by taking in the one-loop of the nucleon. In the context of the chiral partner structure, the mass difference between positive-parity meson and negative-parity meson is generated by the spontaneous breakdown of chiral symmetry. Therefore, I study the masses of $\bar{D}$ (0^-) meson and $\bar{D}_0^*$ (0^+) meson, and the resultant density dependence of them are plotted in Fig. 4.5. In obtaining the result, I include Hartree-type and Fock-type one loop-corrections as well as the mean field contribution. Fig. 4.5 shows that mass of $\bar{D}$ meson increases while that

of $\bar{D}_0^*$ meson decreases. Accordingly, the mass difference between $\bar{D}_0^*$ and $\bar{D}$ mesons gets small. These behaviors fully reflect the partial restoration of chiral symmetry. The spectral function for $\bar{D}_0^*$ meson at several densities are also studied and the results are shown in Fig. 4.6. I find three peaks in the spectral function which essentially correspond to the $\bar{D}_0^*$ meson resonance, a threshold enhancement and a Landau damping. The peak of $\bar{D}_0^*$ meson resonance gets broadened and its hight gets suppressed as the density increases due to collisions with the nucleons surrounding $\bar{D}_0^*$ meson. Its peak position shifts to the lower energy regime which shows a suppression of $\bar{D}_0^*$ meson mass by the partial restoration of chiral symmetry. The threshold enhancement stands around the threshold of $\bar{D} + \pi$. Its peak position shifts to the higher energy regime and this peak gets remarkably enhanced as we increase the density. This feature suggests that this peak is expected to be a proper probe to explore the partial restoration of chiral symmetry in nuclear matter. This peak is caused by a virtual state or a bound state below the $\bar{D} + \pi$ threshold. The Landau damping purely reflects a medium effect which can be understood as a scattering process diagrammatically shown in Fig. 4.7.

Furthermore, I study the spectral function for $\bar{D}_0^*$ meson in nuclear matter which is described by the parity doublet model to make our analysis more realistic. The parity doublet model can reproduce properties of normal nuclear matter in addition to vacuum properties in a consistent way [37, 38]. I should note that a chiral invariant mass m_0 remains as a parameter in this model. The chiral invariant mass is defined by a part of the nucleon mass which is invariant in terms of chiral symmetry. Therefore, the determination of the value of chiral invariant mass is corresponding to seeking the origin of nucleon mass. The spectral functions for $\bar{D}_0^*$ meson for several values of m_0 at $\rho_B = 0.16$ fm^{-3} is indicated in Fig. 5.3. I find clear two peaks in the spectral function which are regarded as the resonance state of $\bar{D}_0^*$ meson and the threshold enhancement. As we increase the value of m_0, the peak position of the resonance shifts to the lower energy regime while that of the threshold enhancement shifts to the higher energy regime. These behaviors claim that the magnitude of the partial restoration of chiral symmetry is strengthened as we increase the value of m_0. These characteristic structures, especially the threshold enhancement, provide us with fruitful information of the strength of partial restoration of chiral symmetry in nuclear matter and the value of m_0, i.e., the origin of mass of the nucleon.

Experimentally, I expect that $\bar{D}_0^*$ mesons in nuclear matter is realized in a nuclear reaction process, e.g.,

$$\bar{p} + A \to D + (\bar{D}_0^* \text{ in medium}) \ . \tag{6.1}$$

According to the Green function's method [47], a (density averaged) spectral function

in nuclear matter is directly reflected into the double differential cross section of the reaction in Eq. (6.1) via a following relation:

$$\frac{d^2\sigma}{dE_D d\Omega} = \left(\frac{d\sigma}{d\Omega}\right)_{\bar{p}+N\to D+\bar{D}_0^*} \times S_{\bar{D}_0^*}(E_{\bar{p}} + E_i - E_D) \ . \tag{6.2}$$

$E_{\bar{p}}$, E_D and E_i are the energy of an incident anti-proton $\bar{p}$, an emitted D meson and the target nucleus A. $S_{\bar{D}_0^*}(E_{\bar{p}} + E_i - E_D)$ is the density averaged spectral function for $\bar{D}_0^*$ captured in the nucleus. $\left(\frac{d\sigma}{d\Omega}\right)_{\bar{p}+N\to D+\bar{D}_0^*}$ is a differential cross section for the elementary process of $\bar{p} + N \to D + \bar{D}_0^*$. The reaction process in Eq. (6.1) can be realized in the future experiment at FAIR and/or J-PARC. Therefore, I need to evaluate the differential cross section in Eq. (6.2) by means of the spectral function for $\bar{D}_0^*$ in Fig. 5.3 in order to complete our quest for the partial restoration of chiral symmetry in nuclear matter and the origin of nucleon mass.

Acknowledgments

Special thanks are due to my supervisor Prof. Masayasu Harada for his invaluable support during my graduate school. Also, I would like to thank to H-ken members for fruitful discussions. This work is supported partly by the Grant-in-Aid for JSPS Research Fellow No. 17J05638.

Appendix A

Finite density field theory

In this appendix, I show derivations of several relations employed in this dissertation in association with the Finite Density Field Theory [42].

A.1 In-medium propagator of a fermion

Here, I show an in-medium propagator of a fermion. Let us prepare a quantized fermion field $\psi(x_0, \vec{x})$ forming a Fermi sea. It is more useful to expand the fermion field $\psi(x_0, \vec{x})$ in terms of its momentum and spin as

$$\psi(x_0, \vec{x}) = \sum_s \int \frac{d^3k}{(2\pi)^3 2\omega_k} \left[b_{k,s} u(\vec{k}, s) \mathrm{e}^{-ik\cdot x} + d^\dagger_{k,s} v(\vec{k}, s) \mathrm{e}^{ik\cdot x} \right] . \tag{A.1}$$

In Eq. (A.1), $\omega_k = \sqrt{|\vec{k}|^2 + m_\psi^2}$ with m_ψ being the mass of ψ represents the energy of the fermion. $b_{k,s}$ and $d^\dagger_{k,s}$ are an annihilation operator of a particle and a creation operator of an anti-particle, respectively, and the index s refers to the spin degrees of freedom. $u(\vec{k}, s)$ and $v(\vec{k}, s)$ are the four components spinors for the particle and anti-particle, respectively, and the four dimensional inner product $k \cdot x$ is defined by $k \cdot x = \omega_k x_0 - \vec{k} \cdot \vec{x}$. $b_{k,s}$ and $d^\dagger_{k,s}$ satisfy following occupation conditions

$$\begin{aligned} \langle b^\dagger_{k,s} b_{k',s'} \rangle &= (2\pi)^3 2\omega_k \theta(k_F - |\vec{k}|) \delta^3(\vec{k} - \vec{k}') \delta_{ss'} \\ \langle d_{k,s} d^\dagger_{k',s'} \rangle &= (2\pi)^3 2\omega_k \delta^3(\vec{k} - \vec{k}') \delta_{ss'} , \end{aligned} \tag{A.2}$$

since the fermion ψ forms the Fermi sea described by the Fermi momentum k_F, where the bracket $\langle \cdots \rangle$ is defined by the average in the presence of the Fermi sea.

The quantization condition for the fermion field in terms of creation and annihilation operators are given by

$$\begin{aligned}
&\{\, b_{k,s}, b^\dagger_{k',s'} \,\} = \{\, d_{k,s}, d^\dagger_{k',s'} \,\} = (2\pi)^3 2\omega_k \delta^3(\vec{k}-\vec{k}')\delta_{ss'} \\
&\{\, b_{k,s}, d^\dagger_{k',s'} \,\} = \{\, d_{k,s}, b^\dagger_{k',s'} \,\} = 0 \ .
\end{aligned} \tag{A.3}$$

Then, a propagator of ψ is straightforwardly evaluated as

$$\begin{aligned}
& \langle \mathrm{T}\psi_\alpha(x)\bar{\psi}_\beta(y)\rangle \\
= \ & \theta(x^0-y^0)\sum_{s,s'}\int \frac{d^3k}{(2\pi)^3 2\omega_k}\frac{d^3k'}{(2\pi)^3 2\omega_{k'}} \langle b_{k,s} b^\dagger_{k',s'}\rangle u_\alpha(\vec{k},s)\bar{u}_\beta(\vec{k}',s')\mathrm{e}^{-ik\cdot x+ik'\cdot y} \\
+ \ & \theta(x^0-y^0)\sum_{s,s'}\int \frac{d^3k}{(2\pi)^3 2\omega_k}\frac{d^3k'}{(2\pi)^3 2\omega_{k'}} \langle d^\dagger_{k,s} d_{k',s'}\rangle v_\alpha(\vec{k},s)\bar{v}_\beta(\vec{k}',s')\mathrm{e}^{ik\cdot x-ik'\cdot y} \\
- \ & \theta(y^0-x^0)\sum_{s,s'}\int \frac{d^3k}{(2\pi)^3 2\omega_k}\frac{d^3k'}{(2\pi)^3 2\omega_{k'}} \langle b^\dagger_{k',s'} b_{k,s}\rangle \bar{u}_\beta(\vec{k}',s')u_\alpha(\vec{k},s)\mathrm{e}^{ik'\cdot y-ik\cdot x} \\
- \ & \theta(y^0-x^0)\sum_{s,s'}\int \frac{d^3k}{(2\pi)^3 2\omega_k}\frac{d^3k'}{(2\pi)^3 2\omega_{k'}} \langle d_{k',s'} d^\dagger_{k,s}\rangle \bar{v}_\beta(\vec{k}',s')v_\alpha(\vec{k},s)\mathrm{e}^{-ik'\cdot y+ik\cdot x} \\
= \ & \theta(x^0-y^0)\int \frac{d^3k}{(2\pi)^3 2\omega_k}(1-\theta(k_F-|\vec{k}|))\Lambda^+_{\alpha\beta}(\vec{k})\mathrm{e}^{-ik\cdot(x-y)} \\
- \ & \theta(y^0-x^0)\int \frac{d^3k}{(2\pi)^3 2\omega_k}\theta(k_F-|\vec{k}|)\Lambda^+_{\alpha\beta}(\vec{k})\mathrm{e}^{-ik\cdot(x-y)} \\
- \ & \theta(y^0-x^0)\int \frac{d^3k}{(2\pi)^3 2\omega_k}\Lambda^-_{\alpha\beta}(\vec{k})\mathrm{e}^{ik\cdot(x-y)} \ ,
\end{aligned} \tag{A.4}$$

where we have defined projection operators

$$\Lambda^\pm_{\alpha\beta}(\vec{k}) = (\not{k} \pm m)_{\alpha\beta} \tag{A.5}$$

with $k_0 = \omega_k$. By using the Fourier transformation of the Heaviside's step function

$$\theta(x_0) = i\int \frac{dk_0}{2\pi}\frac{\mathrm{e}^{-ik_0 t}}{k_0+i\epsilon} \ , \tag{A.6}$$

the in-medium propagator in Eq. (A.4) is further simplified as

$$\begin{aligned}
&\langle \mathrm{T}\psi_\alpha(x)\bar{\psi}_\beta(y)\rangle \\
&= i\int \frac{d^4k}{(2\pi)^4}\left\{\frac{\not{k}+m_\psi}{k^2-m_\psi^2+i\epsilon}+\theta(k_F-|\vec{k}|)\frac{\omega_k\gamma^0-\vec{k}\cdot\gamma+m_\psi}{2\omega_k}\frac{2i\epsilon}{(k_0-\omega_k)^2+\epsilon^2}\right\}\mathrm{e}^{-ik\cdot(x-y)} \\
&= \int \frac{d^4k}{(2\pi^4)}(\not{k}+m_\psi)\left[\frac{i}{k^2-m_\psi^2+i\epsilon}-2\pi\theta(k_0)\theta(k_F-|\vec{k}|)\delta(k^2-m_\psi^2)\right]\mathrm{e}^{-ik\cdot(x-y)}\ .
\end{aligned} \tag{A.7}$$

In obtaining the second equality in Eq. (A.7), we have used

$$\begin{aligned}
\frac{1}{2\omega_k}\frac{2\epsilon}{(k_0-\omega)^2+\epsilon^2} &= \frac{1}{2\omega_k}2\pi\delta(k_0-\omega_k) \\
&= 2\pi\delta(k^2-m_\psi^2)\Big|_{k_0=\omega_k}\ .
\end{aligned} \tag{A.8}$$

Therefore, in the Fourier space, the in-medium fermion propagator is of the form

$$\tilde{G}(k_0,\vec{k}) = \frac{i}{k^2-m_\psi^2+i\epsilon}-2\pi\theta(k_0)\theta(k_F-|\vec{k}|)\delta(k^2-m_\psi^2)\ . \tag{A.9}$$

This expression plays a central role in calculations of nucleon one-loops in nuclear matter.

A.2 Greater and lesser Green's functions (self-energies)

In this section, I summarize relations among greater and lesser Green's function (self-energy), and spectral function.

First, I give a simple expression of spectral function for a spin-0 particle described by a real scalar field $\phi(x_0,\vec{x})$. A propagator of spin-0 particle in the coordinate space $G(x_0,\vec{x})$ is decomposed into a greater part and lesser part as

$$\begin{aligned}
G(x_0,\vec{x}) &= \langle \mathrm{T}\phi(x_0,\vec{x})\phi(0,\vec{0})\rangle \\
&= \theta(x_0)G^>(x_0,\vec{x})+\theta(-x_0)G^<(x_0,\vec{x})\ ,
\end{aligned} \tag{A.10}$$

where we have defined the greater Green's function $G^>(x_0,\vec{x}) = \langle\psi(x_0,\vec{x})\psi(0,\vec{0})\rangle$ and the lesser Green's function $G^<(x_0,\vec{x}) = \langle\psi(0,\vec{0})\psi(x_0,\vec{x})\rangle$. A retarded Green function is defined by

$$G^R(x_0,\vec{x}) = i\theta(x_0)\langle[\psi(x_0,\vec{x}),\psi(0,\vec{0})]\rangle\ , \tag{A.11}$$

and this is represented in terms of $G^{>}(x_0,\vec{x})$ and $G^{<}(x_0,\vec{x})$ as

$$G^R(x_0,\vec{x}) = i\theta(x_0)(G^{>}(x_0,\vec{x}) - G^{<}(x_0,\vec{x})) \ . \tag{A.12}$$

By using the Fourier transformation of the Heaviside's step function in Eq. (A.6), the retarded Green's function in the momentum space in Eq. (A.12) $\tilde{G}^R(q_0,\vec{q})$ takes the form of

$$\begin{aligned}
\tilde{G}^R(q_0,\vec{q}) &= -\int \frac{dk_0}{2\pi} \frac{\tilde{G}^{>}(k_0,\vec{k}) - \tilde{G}^{<}(k_0,\vec{k})}{q_0 - k_0 + i\epsilon} \\
&\equiv -\int \frac{dk_0}{2\pi} \frac{\rho(k_0,\vec{q})}{q_0 - k_0 + i\epsilon} \\
&= -\int \frac{dk_0}{2\pi} \mathrm{P}\, \frac{\rho(k_0,\vec{q})}{q_0 - k_0} + i\frac{1}{2}\rho(q_0,\vec{q}) \ .
\end{aligned} \tag{A.13}$$

In Eq. (A.13), we have defined $\tilde{G}(k_0,\vec{k})$ and $G^{<}(k_0,\vec{k})$ as the Fourier transformation of $G^{>}(x_0,\vec{x})$ and $G^{<}(x_0,\vec{x})$, respectively, and $\rho(k_0,\vec{k})$ is a spectral function for the spin-0 particle defined by

$$\rho(k_0,\vec{k}) \equiv \tilde{G}^{>}(k_0,\vec{k}) - \tilde{G}^{<}(k_0,\vec{k}) \ . \tag{A.14}$$

According to Eq. (A.13), we find a simple relation between the retarded Green's function and the spectral function as

$$\rho(q_0,\vec{q}) = 2\mathrm{Im}\tilde{G}^R(q_0,\vec{q}) \ . \tag{A.15}$$

Also, we can get another relation

$$\mathrm{Im}\tilde{G}^R(q_0,\vec{q}) = \frac{1}{2}\left(\tilde{G}^{>}(q_0,\vec{q}) - \tilde{G}^{<}(q_0,\vec{q})\right) \tag{A.16}$$

from Eqs. (A.15) and (A.14).

In the same manner, a self-energy in the coordinate space $\Sigma(x_0,\vec{x})$ is decomposed as

$$\Sigma(x_0,\vec{x}) = \theta(x_0)\Sigma^{>}(x_0,\vec{x}) + \theta(-x_0)\Sigma^{<}(x_0,\vec{x}) \ , \tag{A.17}$$

where we have defined a greater self-energy $\Sigma^{>}(x_0,\vec{x})$ and a lesser self-energy $\Sigma^{<}(x_0,\vec{x})$, respectively. A retarded self-energy is defined by

$$\Sigma^R(x_0,\vec{x}) = i\theta(x_0)\left(\Sigma^{>}(x_0,\vec{x}) - \Sigma^{<}(x_0,\vec{x})\right) \ . \tag{A.18}$$

In the following, the Fourier transformation of $\Sigma^R(x_0,\vec{x})$, $\Sigma^>(x_0,\vec{x})$ and $\Sigma^<(x_0,\vec{x})$ are described as $\tilde{\Sigma}^R(q_0,\vec{q})$, $\tilde{\Sigma}^>(q_0,\vec{q})$ and $\tilde{\Sigma}^<(q_0,\vec{q})$. Then, the corresponding retarded Green's function is obtained as

$$\tilde{G}^R(q_0,\vec{q}) = -\frac{1}{q^2 - m_\phi^2 - \tilde{\Sigma}^R(q_0,\vec{q})} \tag{A.19}$$

by including infinite sums of $\tilde{\Sigma}^R(q_0,\vec{q})$. m_ϕ is a mass of the spin-0 particle. According to Eq. (A.15) together with Eq. (A.19), we can find an explicit form of spectral function as

$$\rho(q_0,\vec{q}) = \frac{-2\mathrm{Im}\tilde{\Sigma}^R(q_0,\vec{q})}{\left[q^2 - m^2 - \mathrm{Re}\tilde{\Sigma}^R(q_0,\vec{q})\right]^2 + \left[\mathrm{Im}\tilde{\Sigma}^R(q_0,\vec{q})\right]^2} \ . \tag{A.20}$$

Furthermore, we can obtain another powerful relation as in Eq. (A.16):

$$\mathrm{Im}\tilde{\Sigma}^R(q_0,\vec{q}) = \frac{1}{2}\left(\tilde{\Sigma}^>(q_0,\vec{q}) - \tilde{\Sigma}^<(q_0,\vec{q})\right) \ , \tag{A.21}$$

since we have used only the properties of $\theta(x_0)$ and $\theta(-x_0)$ in obtaining Eq. (A.16).

Next, I derive a dispersion relation often referred to as the Kramers-Kronig relation. Because of the definition of the Heaviside's step function and the retarded self-energy in the coordinate space, we find a trivial equality

$$\Sigma^R(x_0,\vec{x}) = \theta(x_0)\Sigma^R(x_0,\vec{x}) \ . \tag{A.22}$$

This equality is passed down in the momentum space as

$$\begin{aligned}\tilde{\Sigma}^R(q_0,\vec{q}) &= i\int\frac{dk_0}{2\pi}\frac{\tilde{\Sigma}^R(k_0,\vec{q})}{q_0 - k_0 + i\epsilon} \\ &= i\mathrm{P}\int\frac{dk_0}{2\pi}\frac{\tilde{\Sigma}^R(k_0,\vec{q})}{q_0 - k_0} + \frac{1}{2}\tilde{\Sigma}_R(q_0,\vec{q}) \ .\end{aligned} \tag{A.23}$$

Therefore, we get a dispersion relation

$$\begin{aligned}\mathrm{Re}\tilde{\Sigma}^R(q_0,\vec{q}) &= \frac{1}{\pi}\mathrm{P}\int_{-\infty}^{\infty} dz\frac{\mathrm{Im}\tilde{\Sigma}^R(z,\vec{q})}{z - q_0} \ . \\ &= \frac{1}{\pi}\mathrm{P}\int_0^{\infty} dz^2\frac{\mathrm{Im}\tilde{\Sigma}^R(z,\vec{q})}{z^2 - q_0^2} \ ,\end{aligned} \tag{A.24}$$

where we have used $\mathrm{Im}\tilde{\Sigma}^R(q_0,\vec{q}) = \epsilon(q_0)\mathrm{Im}\left(i\tilde{\Sigma}(q_0,\vec{q})\right)$ ($\tilde{\Sigma}(q_0,\vec{q})$ is the Fourier transformation of $\Sigma(x_0,\vec{x})$) in obtaining the second line which is followed by a charge conjugation invariance of the spin-0 particle in medium.

The real part of the (retarded) self-energy is often suffered by a UV divergence. When we have a logarithmic UV divergence, the dispersion relation in Eq. (A.24) should be regularized by replacing as

$$\begin{aligned}
\mathrm{Re}\tilde{\Sigma}^R(q_0,\vec{q}) &= \frac{1}{\pi}\mathrm{P}\int_{-\infty}^{\infty} dz^2 \frac{\mathrm{Im}\tilde{\Sigma}^R(z,\vec{q})}{z^2-q_0^2} \\
&\to \frac{1}{\pi}\mathrm{P}\int_{0}^{\infty} dz^2 \left(\frac{\mathrm{Im}\tilde{\Sigma}^R(z,\vec{q})}{z^2-q_0^2} - \frac{\mathrm{Im}\tilde{\Sigma}^R(z,\vec{q})}{z^2-|\vec{q}|^2-m^2}\right) \\
&= \frac{q^2-m_\phi^2}{\pi}\mathrm{P}\int_{0}^{\infty} dz^2 \frac{\mathrm{Im}\tilde{\Sigma}^R(z,\vec{q})}{(z^2-q_0^2)(z^2-|\vec{q}|^2-m_\phi^2)} ,
\end{aligned} \tag{A.25}$$

where we have used an on-shell renormalization condition as $\mathrm{Re}\tilde{\Sigma}^R(\sqrt{|\vec{q}|^2+m_\phi^2},\vec{q}) = 0$.

Finally, I show an explicit form of the greater and lesser Green's functions in the momentum space $\tilde{G}^>_{\mathrm{free}}(q_0,\vec{q})$ and $\tilde{G}^<_{\mathrm{free}}(q_0,\vec{q})$ in the free space. The quantized spin-0 particle field $\phi(x_0,\vec{x})$ is expanded as

$$\phi(x_0,\vec{x}) = \int \frac{d^3q}{(2\pi)^3 2\epsilon_q}\left\{a_q\,\mathrm{e}^{-iq\cdot x} + a_q^\dagger\,\mathrm{e}^{iq\cdot x}\right\} \tag{A.26}$$

in the vacuum, where $\epsilon_q = \sqrt{|\vec{q}|^2+m_\phi^2}$ is the on-shell energy with the momentum $\vec{k}$ and the inner product $q\cdot x$ is defined by $q\cdot x = \epsilon_q x_0 - \vec{q}\cdot\vec{x}$. a_q and $a_q^\dagger$ are the annihilation and creation operators, respectively. The quantization condition is given in terms of a_q and $a_q^\dagger$ by

$$[\,a_q, a_p^\dagger\,] = (2\pi)^3 2\epsilon_q \delta^3(\vec{q}-\vec{p}) \tag{A.27}$$

so that $\tilde{G}^>_{\mathrm{free}}(x_0,\vec{x})$ is calculated as

$$\begin{aligned}
\tilde{G}^>_{\mathrm{free}}(x_0,\vec{x}) &= \langle 0|\phi(x_0,\vec{x})\phi(y_0,\vec{y})|0\rangle|_{y_0=0,\vec{y}=\vec{0}} \\
&= \int \frac{d^3q}{(2\pi)^3}\frac{1}{2\epsilon_q}\mathrm{e}^{-i\epsilon_q x_0 + i\vec{q}\cdot\vec{x}} \\
&= \int \frac{d^4q}{(2\pi)^4}\frac{2\pi}{2\epsilon_q}\delta(q_0-\epsilon_q)\mathrm{e}^{-iq\cdot x} ,
\end{aligned} \tag{A.28}$$

where the vacuum state $|0\rangle$ is defined by $a_q|0\rangle = 0$. In a similar manner, $\tilde{G}^{<}_{\rm free}(x_0, \vec{x})$ is

$$\begin{aligned}
\tilde{G}^{<}_{\rm free}(x_0, \vec{x}) &= \langle 0|\phi(y_0, \vec{y})\phi(x_0, \vec{x})|0\rangle|_{y_0=0, \vec{y}=\vec{0}} \\
&= \int \frac{d^3q}{(2\pi)^3}\frac{1}{2\epsilon_q} {\rm e}^{+i\epsilon_q x_0 - i\vec{q}\cdot\vec{x}} \\
&= \int \frac{d^4q}{(2\pi)^4}\frac{2\pi}{2\epsilon_q}\delta(q_0+\epsilon_q){\rm e}^{-iq\cdot x} \ . \qquad \text{(A.29)}
\end{aligned}$$

Therefore, we can find

$$\begin{aligned}
\tilde{G}^{>}_{\rm free}(q_0, \vec{q}) &= \frac{2\pi}{2\epsilon_q}\delta(q_0-\epsilon_q) \\
\tilde{G}^{<}_{\rm free}(q_0, \vec{q}) &= \frac{2\pi}{2\epsilon_q}\delta(q_0+\epsilon_q) \ . \qquad \text{(A.30)}
\end{aligned}$$

By using Eq. (A.14), the spectral function in the vacuum is easily obtained as

$$\begin{aligned}
\rho_{\rm free}(q_0, \vec{q}) &= \tilde{G}^{>}_{\rm free}(q_0, \vec{q}) - \tilde{G}^{<}_{\rm free}(q_0, \vec{q}) \\
&= \frac{2\pi}{2\epsilon_q}\delta(q_0-\epsilon_q) - \frac{2\pi}{2\epsilon_q}\delta(q_0+\epsilon_q) \\
&= 2\pi\epsilon(q_0)\delta(q^2-m_\phi^2) \ . \qquad \text{(A.31)}
\end{aligned}$$

Furthermore, Eq. (A.31) allows us to find another useful expressions of $\tilde{G}^{>}_{\rm free}(q_0, \vec{q})$ and $\tilde{G}^{<}_{\rm free}(q_0, \vec{q})$ with respect to the spectral function as

$$\begin{aligned}
\tilde{G}^{>}_{\rm free}(q_0, \vec{q}) &= \theta(q_0)\rho_{\rm free}(q_0, \vec{q}) \\
\tilde{G}^{<}_{\rm free}(q_0, \vec{q}) &= -\theta(-q_0)\rho_{\rm free}(q_0, \vec{q}) \ . \qquad \text{(A.32)}
\end{aligned}$$

This relations still hold even when we access to the finite density

$$\begin{aligned}
\tilde{G}^{>}(q_0, \vec{q}) &= \theta(q_0)\rho(q_0, \vec{q}) \\
\tilde{G}^{<}(q_0, \vec{q}) &= -\theta(-q_0)\rho(q_0, \vec{q}) \ , \qquad \text{(A.33)}
\end{aligned}$$

where we replace the spectral function into a general one $\rho(q_0, \vec{q})$. These equations derived in this section help us in calculations of one-loop corrections to self-energies of $\bar{D}$ mesons in nuclear matter in the main text.

Appendix B

Calculations of the self-energies of σ meson and pion

In this appendix, I show explicit calculations of the self-energies of σ meson and pion in Fig. 3.1 in the linear sigma model, and the self-energy of pion in Fig.5.2 in the parity doublet model.

B.1 The self-energies in Fig. 3.1

According to the propagators of σ meson and pion in Eqs. (3.13) and (3.14), the corresponding self-energies are given by

$$\tilde{\Sigma}_\sigma(q_0,\vec{q}) = 2g^2 \int \frac{\tilde{d}^4k}{(2\pi)^4} \mathrm{tr}\left[\tilde{G}_N(k_0,\vec{k})\tilde{G}_N(k_0-q_0,\vec{k}-\vec{q})\right] \tag{B.1}$$

and

$$\tilde{\Sigma}_\pi(q_0,\vec{q}) = 2g^2 \int \frac{\tilde{d}^4k}{(2\pi)^4} \mathrm{tr}\left[i\gamma_5\tilde{G}_N(k_0,\vec{k})i\gamma_5\tilde{G}_N(k_0-q_0,\vec{k}-\vec{q})\right] \ , \tag{B.2}$$

where the nucleon propagator $\tilde{G}_N(k_0)$ is provided by Eq. (A.9):

$$\tilde{G}(k_0,\vec{k}) = \frac{i}{k^2-m_N^2+i\epsilon} - 2\pi\theta(k_0)\theta(k_kF-|\vec{k}|)\delta(k^2-m_N^2) \ . \tag{B.3}$$

The symbol $\tilde{d}^4k$ is defined by Eq. (3.10).

The real part of the retarded self-energies are calculated as

$$\mathrm{Re}\tilde{\Sigma}^R_\sigma(q_0,\vec{q}) \;=\; \frac{g^2}{2\pi^2}\int_0^{k_F} d|\vec{k}|\frac{|\vec{k}|^2}{E_1}\left\{4-\frac{q_0^2-|\vec{q}|^2-4m_N^2}{2|\vec{k}||\vec{q}|}\ln|A_1|\right\} \tag{B.4}$$

and

$$\mathrm{Re}\tilde{\Sigma}^R_\pi(q_0,\vec{q}) \;=\; \frac{g^2}{2\pi^2}\int_0^{k_F} d|\vec{k}|\frac{|\vec{k}|^2}{E_1}\left\{4-\frac{q_0^2-|\vec{q}|^2}{2|\vec{k}||\vec{q}|}\ln|A_1|\right\}\;, \tag{B.5}$$

where we have defined

$$A_1=\frac{q_0^2-|\vec{q}|^2+2|\vec{k}||\vec{q}|+2q_0E_1}{q_0^2-|\vec{q}|^2-2|\vec{k}||\vec{q}|+2q_0E_1}\frac{q_0^2-|\vec{q}|^2+2|\vec{k}||\vec{q}|-2q_0E_1}{q_0^2-|\vec{q}|^2-2|\vec{k}||\vec{q}|-2q_0E_1} \tag{B.6}$$

and

$$E_1 \;=\; \sqrt{|\vec{k}|^2+m_N^2}\;. \tag{B.7}$$

The imaginary parts of the retarded self-energies are

$$\begin{aligned}
\mathrm{Im}\tilde{\Sigma}^R_\sigma(q_0,\vec{q}) \;&=\; 4\pi g^2(q^2-4m_N^2)\int\frac{d^3k}{(2\pi)^3}\frac{1}{4E_1E_2}\theta(k_F-|\vec{k}|)\delta(q_0-E_1-E_2)\\
&-\; 4\pi g^2(q^2-4m_N^2)\int\frac{d^3k}{(2\pi)^3}\frac{1}{4E_1E_2}\theta(k_F-|\vec{k}|)\delta(q_0+E_1+E_2)\\
&-\; 4\pi g^2(q^2-4m_N^2)\int\frac{d^3k}{(2\pi)^3}\frac{1}{4E_1E_2}\theta(k_F-|\vec{k}|)\delta(q_0-E_1+E_2)\\
&+\; 4\pi g^2(q^2-4m_N^2)\int\frac{d^3k}{(2\pi)^3}\frac{1}{4E_1E_2}\theta(k_F-|\vec{k}|)\delta(q_0+E_1-E_2)
\end{aligned} \tag{B.8}$$

and

$$\begin{aligned}
\mathrm{Im}\tilde{\Sigma}^R_\pi(q_0,\vec{q}) \;&=\; 4\pi g^2q^2\int\frac{d^3k}{(2\pi)^3}\frac{1}{4E_1E_2}\theta(k_F-|\vec{k}|)\delta(q_0-E_1-E_2)\\
&-\; 4\pi g^2q^2\int\frac{d^3k}{(2\pi)^3}\frac{1}{4E_1E_2}\theta(k_F-|\vec{k}|)\delta(q_0+E_1+E_2)\\
&-\; 4\pi g^2q^2\int\frac{d^3k}{(2\pi)^3}\frac{1}{4E_1E_2}\theta(k_F-|\vec{k}|)\delta(q_0-E_1+E_2)\\
&+\; 4\pi g^2q^2\int\frac{d^3k}{(2\pi)^3}\frac{1}{4E_1E_2}\theta(k_F-|\vec{k}|)\delta(q_0+E_1-E_2)\;,
\end{aligned} \tag{B.9}$$

where E_2 is defined by

$$E_2 \;=\; \sqrt{|\vec{k}-\vec{q}|^2+m_N^2}\;. \tag{B.10}$$

Note that $\tilde{\Sigma}_\pi(q_0,\vec{q})$ (or $\tilde{\Sigma}^R_\pi(q_0,\vec{q})$) satisfies $\tilde{\Sigma}_\pi(q_0,\vec{0})=0$ (or $\tilde{\Sigma}^R_\pi(q_0,\vec{0})=0$). This fact allows us to find

$$i\tilde{G}^{ab,-1}_\pi(q_0,\vec{0}) = q_0^2\delta^{ab} \tag{B.11}$$

in a chiral limit $m_\pi \to 0$. Namely, the pion remains massless which clearly shows a behavior of the Nambu-Goldstone boson (NG boson).

B.2 The self-energy in Fig.5.2

Here, I shall show calculations of the self-energies of pion in Fig. 5.2. I simply show the results here. In the following, I define energies of the nucleon and $N^*(1535)$ with momentum $\vec{k}$ by E_k^+ and E_k^-, respectively, as

$$\begin{aligned} E_k^+ &\equiv \sqrt{|\vec{k}|^2+m_+^2} \\ E_k^- &\equiv \sqrt{|\vec{k}|^2+m_-^2}\;. \end{aligned} \tag{B.12}$$

Also, I define following quantities

$$\begin{aligned} A_+ &\equiv \frac{q_0^2-|\vec{q}|^2+2|\vec{k}||\vec{q}|+2q_0E_k^+}{q_0^2-|\vec{q}|^2-2|\vec{k}||\vec{q}|+2q_0E_k^+}\,\frac{q_0^2-|\vec{q}|^2+2|\vec{k}||\vec{q}|-2q_0E_k^+}{q_0^2-|\vec{q}|^2-2|\vec{k}||\vec{q}|-2q_0E_k^+}\;, \\ A_{+-} &\equiv \frac{q_0^2-|\vec{q}|^2+2|\vec{k}||\vec{q}|+m_+^2-m_-^2+2q_0E_k^+}{q_0^2-|\vec{q}|^2-2|\vec{k}||\vec{q}|+m_+^2-m_-^2+2q_0E_k^+}\,\frac{q_0^2-|\vec{q}|^2+2|\vec{k}||\vec{q}|+m_+^2-m_-^2-2q_0E_k^+}{q_0^2-|\vec{q}|^2-2|\vec{k}||\vec{q}|+m_+^2-m_-^2-2q_0E_k^+}\;, \\ A_{-+} &\equiv \frac{q_0^2-|\vec{q}|^2-2q_0E_k^-+2|\vec{k}||\vec{q}|+m_-^2-m_+^2}{q_0^2-|\vec{q}|^2-2q_0E_k^--2|\vec{k}||\vec{q}|+m_-^2-m_+^2}\,\frac{q_0^2-|\vec{q}|^2+2q_0E_k^-+2|\vec{k}||\vec{q}|+m_-^2-m_+^2}{q_0^2-|\vec{q}|^2+2q_0E_k^--2|\vec{k}||\vec{q}|+m_-^2-m_+^2}\;, \\ A_- &\equiv \frac{q_0^2-|\vec{q}|^2+2|\vec{k}||\vec{q}|+2q_0E_k^-}{q_0^2-|\vec{q}|^2-2|\vec{k}||\vec{q}|+2q_0E_k^-}\,\frac{q_0^2-|\vec{q}|^2+2|\vec{k}||\vec{q}|-2q_0E_k^-}{q_0^2-|\vec{q}|^2-2|\vec{k}||\vec{q}|-2q_0E_k^-} \end{aligned} \tag{B.13}$$

for the convenient.

The real part of the sum of retarded self-energies is obtained as

$$\mathrm{Re}\tilde{\Sigma}^R_\pi(q_0,\vec{q}) = \mathrm{Re}\tilde{\Sigma}^R_{\pi,+}(q_0,\vec{q}) + \mathrm{Re}\tilde{\Sigma}^R_{\pi,-}(q_0,\vec{q}) \tag{B.14}$$

where $\mathrm{Re}\tilde{\Sigma}^R_{\pi,+}(q_0,\vec{q})$ and $\mathrm{Re}\tilde{\Sigma}^R_{\pi,-}(q_0,\vec{q})$ are

$$
\begin{aligned}
& \mathrm{Re}\tilde{\Sigma}^R_{\pi,+}(q_0,\vec{q}) \\
= \;& \frac{g^2_{NN\pi}}{2\pi^2}\int_0^{k_{F+}} d|\vec{k}|\frac{|\vec{k}|^2}{E^+_k}\left\{4-\frac{q_0^2-|\vec{q}|^2}{2|\vec{k}||\vec{q}|}\ln|A_+|\right\} \\
- \;& m_+^2\frac{(2\sigma_0 h_{NN\pi})^2}{\pi^2}\int_0^{k_{F+}} d|\vec{k}|\frac{|\vec{k}|^2}{E^+_k}\frac{q_0^2-|\vec{q}|^2}{|\vec{k}||\vec{q}|}\ln|A_+| \\
+ \;& \frac{4\sigma_0 m_+ g_{NN\pi}h_{NN\pi}}{\pi^2}(q_0^2-|\vec{q}|^2)\int_0^{k_{F+}} d|\vec{k}|\frac{|\vec{k}|^2}{E^+_k}\frac{1}{2|\vec{k}||\vec{q}|}\ln|A_+| \\
+ \;& \frac{g^2_{NN^*\pi}}{\pi^2}\int_0^{k_{F+}} d|\vec{k}|\frac{|\vec{k}|^2}{E^+_k}\left\{2-\frac{q_0^2-|\vec{q}|^2-(m_++m_-)^2}{4|\vec{k}||\vec{q}|}\ln|A_{+-}|\right\} \\
+ \;& \frac{2(2\sigma_0 h_{NN^*\pi})^2}{\pi^2}\int_0^{k_{F+}} d|\vec{k}|\frac{|\vec{k}|^2}{2E^+_k}2(m_-^2-m_+^2) \\
- \;& \frac{2(2\sigma_0 h_{NN^*\pi})^2}{\pi^2}\int_0^{k_{F+}} d|\vec{k}|\frac{|\vec{k}|^2}{2E^+_k}\frac{(m_--m_+)^2(q_0^2-|\vec{q}|^2-(m_++m_-)^2)}{4|\vec{k}||\vec{q}|}\ln|A_{+-}| \\
+ \;& \frac{8\sigma_0 g_{NN^*\pi}h_{NN^*\pi}}{\pi^2}\int_0^{k_{F+}} d|\vec{k}|\frac{|\vec{k}|^2}{2E^+_k}2(m_++m_-)\ln|A_{+-}| \\
- \;& \frac{8\sigma_0 g_{NN^*\pi}h_{NN^*\pi}}{\pi^2}\int_0^{k_{F+}} d|\vec{k}|\frac{|\vec{k}|^2}{2E^+_k}\frac{(m_--m_+)(q_0^2-|\vec{q}|^2-(m_++m_-)^2)}{4|\vec{k}||\vec{q}|}\ln|A_{+-}| \\
- \;& \frac{2g_{NN\sigma}m_+}{\pi^2\sigma_0}\int_0^{k_{F+}} d|\vec{k}|\frac{|\vec{k}|^2}{E^+_k}\ , \qquad \text{(B.15)}
\end{aligned}
$$

and

$$
\begin{aligned}
& \mathrm{Re}\tilde{\Sigma}^R_{\pi,-}(q_0,\vec{q}) \\
= \;& \frac{g^2_{N^*N^*\pi}}{2\pi^2}\int_0^{k_{F-}} d|\vec{k}|\frac{|\vec{k}|^2}{E^-_k}\left\{4-\frac{q_0^2-|\vec{q}|^2}{2|\vec{k}||\vec{q}|}\ln|A_-|\right\} \\
- \;& m_-^2\frac{(2\sigma_0 h_{N^*N^*\pi})^2}{\pi^2}\int_0^{k_{F-}} d|\vec{k}|\frac{|\vec{k}|^2}{E^-_k}\frac{q_0^2-|\vec{q}|^2}{|\vec{k}||\vec{q}|}\ln|A_-| \\
+ \;& \frac{4\sigma_0 m_- g_{N^*N^*\pi}h_{N^*N^*\pi}}{\pi^2}(q_0^2-|\vec{q}|^2)\int_0^{k_{F-}} d|\vec{k}|\frac{|\vec{k}|^2}{E^-_k}\frac{1}{2|\vec{k}||\vec{q}|}\ln|A_-| \\
+ \;& \frac{g^2_{NN^*\pi}}{\pi^2}\int_0^{k_{F-}} d|\vec{k}|\frac{|\vec{k}|^2}{E^-_k}\left\{2-\frac{q_0^2-|\vec{q}|^2-(m_++m_-)^2}{4|\vec{k}||\vec{q}|}\ln|A_{-+}|\right\} \\
+ \;& \frac{2(2\sigma_0 h_{NN^*\pi})^2}{\pi^2}\int_0^{k_{F-}} d|\vec{k}|\frac{|\vec{k}|^2}{2E^-_k}2(m_-^2-m_+^2) \\
- \;& \frac{2(2\sigma_0 h_{NN^*\pi})^2}{\pi^2}\int_0^{k_{F-}} d|\vec{k}|\frac{|\vec{k}|^2}{2E^-_k}\frac{(m_--m_+)^2(q_0^2-|\vec{q}|^2-(m_++m_-)^2)}{4|\vec{k}||\vec{q}|}\ln|A_{-+}| \\
- \;& \frac{8\sigma_0 g_{NN^*\pi}h_{NN^*\pi}}{\pi^2}\int_0^{k_{F-}} d|\vec{k}|\frac{|\vec{k}|^2}{2E^-_k}2(m_++m_-)\ln|A_{-+}| \\
- \;& \frac{8\sigma_0 g_{NN^*\pi}h_{NN^*\pi}}{\pi^2}\int_0^{k_{F-}} d|\vec{k}|\frac{|\vec{k}|^2}{2E^-_k}\frac{(m_--m_+)(q_0^2-|\vec{q}|^2-(m_++m_-)^2)}{4|\vec{k}||\vec{q}|}\ln|A_{-+}| \\
- \;& \frac{2g_{N^*N^*\sigma}m_-}{\pi^2\sigma_0}\int_0^{k_{F-}} d|\vec{k}|\frac{|\vec{k}|^2}{E^-_k}\ , \qquad \text{(B.16)}
\end{aligned}
$$

respectively.

The imaginary part also has two parts as

$$
\mathrm{Im}\tilde{\Sigma}^R_{\pi}(q_0,\vec{q}) = \mathrm{Im}\tilde{\Sigma}^R_{\pi,+}(q_0,\vec{q}) + \mathrm{Im}\tilde{\Sigma}^R_{\pi,-}(q_0,\vec{q})\ , \qquad \text{(B.17)}
$$

where $\mathrm{Im}\tilde{\Sigma}^R_{\pi,+}(q_0,\vec{q})$ is

$$
\begin{aligned}
& \mathrm{Im}\tilde{\Sigma}^R_{\pi,+}(q_0,\vec{q}) \\
= \;& \pi G_1^2 \frac{q_0^2-|\vec{q}|^2}{2}\int \frac{d^3k}{(2\pi)^3}\frac{1}{E_k^+E_{k-q}^+}\theta(k_{F+}-|\vec{k}|)\delta(q_0-E_k^+-E_{k-q}^+) \\
- \;& \pi G_1^2 \frac{q_0^2-|\vec{q}|^2}{2}\int \frac{d^3k}{(2\pi)^3}\frac{1}{E_k^+E_{k-q}^+}\theta(k_{F+}-|\vec{k}|)\delta(q_0+E_k^++E_{k-q}^+) \\
- \;& \pi G_1^2 \frac{q_0^2-|\vec{q}|^2}{2}\int \frac{d^3k}{(2\pi)^3}\frac{1}{E_k^+E_{k-q}^+}\theta(k_{F+}-|\vec{k}|)\delta(q_0-E_k^++E_{k-q}^+) \\
+ \;& \pi G_1^2 \frac{q_0^2-|\vec{q}|^2}{2}\int \frac{d^3k}{(2\pi)^3}\frac{1}{E_k^+E_{k-q}^+}\theta(k_{F+}-|\vec{k}|)\delta(q_0+E_k^+-E_{k-q}^+) \\
+ \;& \pi G_2^2 \frac{q_0^2-|\vec{q}|^2-(m_++m_-)^2}{2}\int \frac{d^3k}{(2\pi)^3}\frac{1}{E_k^+E_{k-q}^-}\theta(k_{F+}-|\vec{k}|)\delta(q_0-E_k^+-E_{k-q}^-) \\
- \;& \pi G_2^2 \frac{q_0^2-|\vec{q}|^2-(m_++m_-)^2}{2}\int \frac{d^3k}{(2\pi)^3}\frac{1}{E_{k-q}^-E_k^+}\theta(k_{F+}-|\vec{k}|)\delta(q_0+E_{k-q}^-+E_k^+) \\
- \;& \pi G_2^2 \frac{q_0^2-|\vec{q}|^2-(m_++m_-)^2}{2}\int \frac{d^3k}{(2\pi)^3}\frac{1}{E_k^+E_{k-q}^-}\theta(k_{F+}-|\vec{k}|)\delta(q_0-E_k^++E_{k-q}^-) \\
+ \;& \pi G_2^2 \frac{q_0^2-|\vec{q}|^2-(m_++m_-)^2}{2}\int \frac{d^3k}{(2\pi)^3}\frac{1}{E_{k-q}^-E_k^+}\theta(k_{F+}-|\vec{k}|)\delta(q_0-E_{k-q}^-+E_k^+)\ ,
\end{aligned}
\tag{B.18}
$$

and $\mathrm{Im}\tilde{\Sigma}^R_{\pi,-}(q_0,\vec{q})$ is

$$
\begin{aligned}
& \mathrm{Im}\tilde{\Sigma}^R_{\pi,-}(q_0,\vec{q}) \\
= \;& \pi G_3^2 \frac{q_0^2-|\vec{q}|^2}{2}\int\frac{d^3k}{(2\pi)^3}\frac{1}{E_k^- E_{k-q}^-}\theta(k_{F-}-|\vec{k}|)\delta(q_0-E_k^- - E_{k-q}^-) \\
- \;& \pi G_3^2 \frac{q_0^2-|\vec{q}|^2}{2}\int\frac{d^3k}{(2\pi)^3}\frac{1}{E_k^- E_{k-q}^-}\theta(k_{F-}-|\vec{k}|)\delta(q_0+E_k^- + E_{k-q}^-) \\
- \;& \pi G_3^2 \frac{q_0^2-|\vec{q}|^2}{2}\int\frac{d^3k}{(2\pi)^3}\frac{1}{E_k^- E_{k-q}^-}\theta(k_{F-}-|\vec{k}|)\delta(q_0-E_k^- + E_{k-q}^-) \\
+ \;& \pi G_3^2 \frac{q_0^2-|\vec{q}|^2}{2}\int\frac{d^3k}{(2\pi)^3}\frac{1}{E_k^- E_{k-q}^-}\theta(k_{F-}-|\vec{k}|)\delta(q_0+E_k^- - E_{k-q}^-) \\
+ \;& \pi G_2^2 g^2 \frac{q_0^2-|\vec{q}|^2-(m_++m_-)^2}{2}\int\frac{d^3k}{(2\pi)^3}\frac{1}{E_k^- E_{k-q}^+}\theta(k_{F-}-|\vec{k}|)\delta(q_0-E_k^- - E_{k-q}^+) \\
- \;& \pi G_2^2 \frac{q_0^2-|\vec{q}|^2-(m_++m_-)^2}{2}\int\frac{d^3k}{(2\pi)^3}\frac{1}{E_{k-q}^+ E_k^-}\theta(k_{F-}-|\vec{k}|)\delta(q_0+E_{k-q}^+ + E_k^-) \\
- \;& \pi G_2^2 \frac{q_0^2-|\vec{q}|^2-(m_++m_-)^2}{2}\int\frac{d^3k}{(2\pi)^3}\frac{1}{E_k^- E_{k-q}^+}\theta(k_{F-}-|\vec{k}|)\delta(q_0-E_k^- + E_{k-q}^+) \\
+ \;& \pi G_2^2 \frac{q_0^2-|\vec{q}|^2-(m_++m_-)^2}{2}\int\frac{d^3k}{(2\pi)^3}\frac{1}{E_{k-q}^+ E_k^-}\theta(k_{F-}-|\vec{k}|)\delta(q_0-E_{k-q}^+ + E_k^-)\ .
\end{aligned}
\tag{B.19}
$$

In these expressions, the couplings G_1, G_2 and G_3 are defined by

$$
\begin{aligned}
G_1 &\equiv g_{NN\pi} + 4\sigma_0 m_+ h_{NN\pi}\ , && \text{(B.20)}\\
G_2 &\equiv g_{NN^*\pi} + 2\sigma_0(m_- - m_+)h_{NN^*\pi}\ , && \text{(B.21)}\\
G_3 &\equiv g_{N^*N^*\pi} + 4\sigma_0 m_- h_{N^*N^*\pi}\ . && \text{(B.22)}
\end{aligned}
$$

Again we can confirm $\tilde{\Sigma}_\pi(q_0,\vec{q})$ with $\vec{q}\to\vec{0}$ in a chiral limit together with the gap equation in Eq. (5.23), which indicates that pion becomes massless.

References

[1] Y. Nambu and G. Jona-Lasinio, Phys. Rev. **122**, 345 (1961).

[2] Y. Nambu and G. Jona-Lasinio, Phys. Rev. **124**, 246 (1961).

[3] S. Weinberg, Phys. Rev. Lett. **19**, 1264 (1967).

[4] A. Salam, in *Elementaly Particle Theory*, ed. by N. Svartholom (Almquist and Forlag, 1968) p. 367

[5] S. R. Coleman, J. Wess and B. Zumino, Phys. Rev. **177**, 2239 (1969). doi:10.1103/PhysRev.177.2239

[6] C. G. Callan, Jr., S. R. Coleman, J. Wess and B. Zumino, Phys. Rev. **177**, 2247 (1969). doi:10.1103/PhysRev.177.2247

[7] J. Gasser and H. Leutwyler, Annals Phys. **158**, 142 (1984). doi:10.1016/0003-4916(84)90242-2

[8] J. Gasser and H. Leutwyler, Nucl. Phys. B **250**, 465 (1985). doi:10.1016/0550-3213(85)90492-4

[9] For a review, see, e.g., Ref. [10] for the inhomogeneous chiral phase and Ref. [11] for the restoration of chiral symmetry in medium.

[10] M. Buballa and S. Carignano, Prog. Part. Nucl. Phys. **81**, 39 (2015) doi:10.1016/j.ppnp.2014.11.001 [arXiv:1406.1367 [hep-ph]].

[11] T. Hatsuda and T. Kunihiro, Phys. Rept. **247**, 221 (1994) doi:10.1016/0370-1573(94)90022-1.

[12] C. DeTar and U. M. Heller, Eur. Phys. J. A **41**, 405 (2009) doi:10.1140/epja/i2009-10825-3 [arXiv:0905.2949 [hep-lat]].

[13] R. S. Hayano and T. Hatsuda, Rev. Mod. Phys. **82**, 2949 (2010).

[14] D. Suenaga, B. R. He, Y. L. Ma and M. Harada, Phys. Rev. C **89**, no. 6, 068201 (2014) doi:10.1103/PhysRevC.89.068201 [arXiv:1403.5140 [hep-ph]].

[15] D. Suenaga, B. R. He, Y. L. Ma and M. Harada, Phys. Rev. D **91**, no. 3, 036001 (2015) doi:10.1103/PhysRevD.91.036001 [arXiv:1412.2462 [hep-ph]].

[16] D. Suenaga and M. Harada, Phys. Rev. D **93**, no. 7, 076005 (2016) doi:10.1103/PhysRevD.93.076005 [arXiv:1509.08578 [hep-ph]].

[17] M. Harada, Y. L. Ma, D. Suenaga and Y. Takeda, PTEP 2017, no. 11, 113D01 (2017).

[18] D. Suenaga, S. Yasui and M. Harada, Phys. Rev. C **96**, no. 1, 015204 (2017) doi:10.1103/PhysRevC.96.015204 [arXiv:1703.02762 [nucl-th]].

[19] M. Neubert, Phys. Rept. **245**, 259 (1994).

[20] A.V. Manohar and M.B. Wise, Camb. Monogr. Part. Phys. Nucl. Phys. Cosmol. **10**, 1 (2000).

[21] R. Casalbuoni, A. Deandrea, N. Di Bartolomeo, R. Gatto, F. Feruglio and G. Nardulli, Phys. Rept. **281**, 145 (1997).

[22] K. Tsushima, D. H. Lu, A. W. Thomas, K. Saito and R. H. Landau, Phys. Rev. C **59**, 2824 (1999) doi:10.1103/PhysRevC.59.2824.

[23] A. Hayashigaki, Phys. Lett. B **487**, 96 (2000) doi:10.1016/S0370-2693(00)00760-7.

[24] T. Hilger, R. Thomas and B. Kampfer, Phys. Rev. C **79**, 025202 (2009) doi:10.1103/PhysRevC.79.025202.

[25] K. Azizi, N. Er and H. Sundu, Eur. Phys. J. C **74**, 3021 (2014) doi:10.1140/epjc/s10052-014-3021-1.

[26] Z. G. Wang, Phys. Rev. C **92**, no. 6, 065205 (2015) doi:10.1103/PhysRevC.92.065205.

[27] K. Suzuki, P. Gubler and M. Oka, Phys. Rev. C **93**, no. 4, 045209 (2016) doi:10.1103/PhysRevC.93.045209.

[28] M. F. M. Lutz and C. L. Korpa, Phys. Lett. B **633**, 43 (2006) doi:10.1016/j.physletb.2005.11.046.

[29] L. Tolos, A. Ramos and T. Mizutani, Phys. Rev. C **77**, 015207 (2008) doi:10.1103/PhysRevC.77.015207.

[30] C. E. Jimenez-Tejero, A. Ramos, L. Tolos and I. Vidana, Phys. Rev. C **84**, 015208 (2011) doi:10.1103/PhysRevC.84.015208.

[31] C. Garcia-Recio, J. Nieves, L. L. Salcedo and L. Tolos, Phys. Rev. C **85**, 025203 (2012).

[32] A. Mishra, E. L. Bratkovskaya, J. Schaffner-Bielich, S. Schramm and H. Stocker, Phys. Rev. C **69**, 015202 (2004).

[33] A. Kumar and A. Mishra, Phys. Rev. C **81**, 065204 (2010) doi:10.1103/PhysRevC.81.065204.

[34] S. Yasui and K. Sudoh, Phys. Rev. C **87**, no. 1, 015202 (2013) doi:10.1103/PhysRevC.87.015202.

[35] J. S. Schwinger, Annals Phys. **2**, 407 (1957).

[36] M. Gell-Mann and M. Levy, Nuovo Cim. **16**, 705 (1960).

[37] Y. Motohiro, Y. Kim and M. Harada, Phys. Rev. C **92**, no. 2, 025201 (2015) Erratum: [Phys. Rev. C **95**, no. 5, 059903 (2017)] doi:10.1103/PhysRevC.92.025201, 10.1103/PhysRevC.95.059903 [arXiv:1505.00988 [nucl-th]].

[38] D. Suenaga, arXiv:1704.03630 [nucl-th].

[39] M. A. Nowak, M. Rho and I. Zahed, Phys. Rev. D **48**, 4370 (1993) doi:10.1103/PhysRevD.48.4370.

[40] W. A. Bardeen and C. T. Hill, Phys. Rev. D **49**, 409 (1994).

[41] M. C. Birse, J. Phys. G **20**, 1537 (1994) doi:10.1088/0954-3899/20/10/003.

[42] See, e.g., M. Le Bellac, "*Thermal Field Theory*", Cambridge Monographs On Mathematical Physics (2000), and A. L. Fetter and J. D. Walecka, "*Quantum Theory of Many-Particle Systems*", Dover Publications, INC. (2002).

[43] C. E. DeTar and T. Kunihiro, Phys. Rev. D **39**, 2805 (1989).

[44] Y. Nemoto, D. Jido, M. Oka and A. Hosaka, Phys. Rev. D **57**, 4124 (1998).

[45] D. Jido, Y. Nemoto, M. Oka and A. Hosaka, Nucl. Phys. A **671**, 471 (2000).

[46] D. Jido, M. Oka and A. Hosaka, Prog. Theor. Phys. **106**, 873 (2001).

[47] O. Morimatsu and K. Yazaki, Nucl. Phys. A **435**, 727 (1985). doi:10.1016/0375-9474(85)90185-X